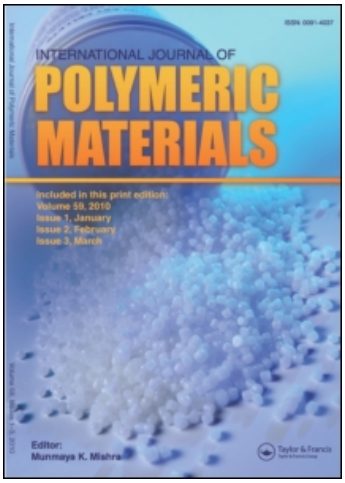

International Journal of Polymeric Materials
Publication details, including instructions for authors and subscription information:
http://www.informaworld.com/smpp/title~content=t713647664

Effect of Polymer Matrix on Kinetics and Mechanism of Carbene Reactions

E. Ya. Davydov[a]; A. P. Vorotnikov[a]; V. P. Pustoshny[a]; G. E. Zaikov[a]
[a] Institute of Biochemical Physics RAN, Moscow, Russia

To cite this Article Davydov, E. Ya. , Vorotnikov, A. P. , Pustoshny, V. P. and Zaikov, G. E.(1997) 'Effect of Polymer Matrix on Kinetics and Mechanism of Carbene Reactions', International Journal of Polymeric Materials, 37: 1, 75 — 131
To link to this Article: DOI: 10.1080/00914039708031479
URL: http://dx.doi.org/10.1080/00914039708031479

Intern. J. Polymeric Mater., 1997, Vol. 37, pp. 75–131
Reprints available directly from the publisher
Photocopying permitted by license only

Effect of Polymer Matrix on Kinetics and Mechanism of Carbene Reactions

E. YA. DAVYDOV, A. P. VOROTNIKOV,
V. P. PUSTOSHNY and G. E. ZAIKOV

Institute of Biochemical Physics RAN, Moscow, Russia

(Received 10 September 1996)

The features of kinetics and mechanism of the cage radical reactions initiated by carbenes in solid polymers has been considered. The peculiar low temperature reaction of arylcarbenes is their interaction in clusters with formation of biradicals (BR). The yield of BR is a measure of the distribution non-homogeneity of the carbene precursors in polymers. The reaction of BR formation allows us to study the molecular dynamics at cryogenic temperatures. The main factor determining the kinetic non-equivalence of triplet carbenes in low temperature reaction of the hydrogen atom abstraction is the dispersion of the cage distances between carbenes and C—H bonds of macromolecules. The strong effect of structural modifications in filled polymers on the thermal decay of carbenes has been established. The matrix effect on the mechanism of the product formation in the carbene reactions, associated with the relaxation processes, has been recognized by the example of the polyvinylalcohol cross-linkage. The advantage of polyisoprene stabilization against thermoxidation by the phenol grafting in carbene synthesis has been shown.

Keywords: Carbene reactions; cage radicals; kinetics; thermoxidation; matrix effects; hydrogen abstraction

INTRODUCTION

The carbene reactions are currently used to develop polymeric materials with required mechanical, chemical, ecological purposes [1–3]. The advantages of such reactions are the mild conditions under which they take place. The most general-purpose techniques of the carbene generation are thermal, thermocatalytic and photodecompositions of diazocompounds. The thermal decomposition of diazocompounds is conducted at

moderate temperatures of 80–100°C. It has been found that the mechanism of the carbene reactions in frozen organic compounds differs essentially from that in liquids and gasses. These features are due to the fundamental property of the solid phase reactions that lies in the dependence of reactivity on the physical structure of the matrix [4].

In spite of considerable scientific material relative to carbene reactions in gaseous and liquid phase the quantitative kinetic data of these processes in solid polymers are very limited. The question of the polymer matrix effect on the carbene reactivity require closer examination. The distinctive characteristic of solid polymers is the structural physical non-homogeneity that effects the composition of products and kinetics of carbene reaction. Therefore, the structural non-homogeneity can lead to a ununiform distribution of the low molecular additives, such as diazocompounds. This in turn can effect the efficiency of the competitive carbene reactions: recombination or reaction with macromolecules. Another possible manifestation of the structural non-homogeneity of polymers is the wide distribution of frequencies and amplitudes of molecular motions [5] and mutual space configurations of reacting carbenes and chemical bonds of macromolecules.

These factors explain the influence of polymer phase on the kinetics and the mechanism of the carbene reactions. In turn the peculiarities of the mechanism of these reactions contain information relative to the molecular organization of polymers on the cage surrounding level. In this connection the investigation of the carbene reaction mechanism and the composition of resulting products offer the possibilities to study the microstructure of polymers. These studies require the development of methods to modify polymers by grafting of different functional groups on macromolecules. This approach allows us to solve the questions of the influence mechanism of polymer medium on the reactivity in the cage reactions, the nature of kinetic non-equivalence in the elementary reactions of the hydrogen atom transfer and reactions involving the radical pairs (RP).

THE SOLID PHASE EFFECT ON THE MECHANISM OF THE CARBENE REACTIONS

The carbene reactivity is determined by the spin state [6]. The singlet carbene can be inserted into ordinary chemical bonds by the one-step

process and stereospecifically added to alkenes with the cyclopropane formation

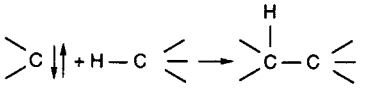

(1)

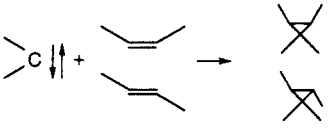

(2)

The spin retention rule for triplet carbene forbids the one-step interaction. The addition of triplet carbenes to alkenes takes place unstereospecifically because of rotation around C—C bond is faster than intersystem conversion [7].

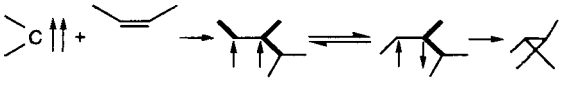

(3)

The reaction of triplet carbenes with C—H bonds results in the RP formation that can recombine by conversion in singlet state.

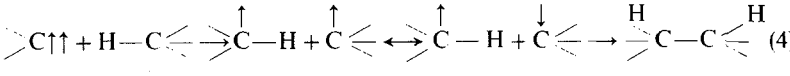

(4)

Formally in the general view the carbene conversions can be presented as follows [8]

$$>C{=}N{=}N$$

$$-N_2 \downarrow h\nu, kT$$

$$\text{products} \xleftarrow{k_1} >C\uparrow\downarrow \underset{k_{TS}}{\overset{k_{ST}}{\rightleftharpoons}} >C\uparrow\uparrow \xrightarrow{k_2} \text{products} \qquad (5)$$

The transition from gas and liquids to frozen organic matrices must provide the relaxation of carbenes from the excited singlet state into the ground triplet state and consequently the increase of the carbene

conversion efficiency by the abstract-recombination mechanism (4). The matrix effect of such type was observed for reactions of carbenes with alkenes [9] and alcohols [10]. By the change of the phase state not only the spin state of carbenes, but the structural-physical characteristics (volume, form of the matrix molecules and carbene precursors) can exhibit effect on kinetics and the product composition. In this connection the investigations directed to the elucidation of the role of the mutual spatial arrangement of the carbene centre and its surroundings are most interesting for the carbene reactions in rigid matrix.

The dramatic example of the space-orientation effect on the carbene chemistry is the dependence of selectivity for reactions of the diphenylcarbene (DPC) insertion into different C—H bonds of isopropanol at 77 K on the nature of the carbene precursor [11]. This is evident from the space-configuration correspondence of the carbene precursor and the matrix molecules of alcohol, from their relative sizes.

The characteristic feature of the cage reaction of the thermal decay of triplet carbenes in solids connected with the hydrogen atom transfer from surrounding molecules to carbenes is the kinetic non-equivalence of particles. Because of this the kinetics of DPC decay in frozen glasses (77 K) depends on the duration of their photochemical producing stage [12]. The effective rate constant of the carbene decay decreases as the photolysis time increases. The explanation must be invoked to account for this result within the limits of concepts about the structural non-homogeneity of the reaction cages of matrix. The reactivity of carbenes depends on the located orientations in cages, in so doing each orientation coresponds to the distinct rate constant k_1. In the reacting system the distribution by the rate constants is steadily changed as the disappearance of the most favourable orientations for reaction takes place. Because of the strong hindering of molecular movements at low temperatures the favourable carbene orientations are not regenerated and the distribution becomes less and less active.

The special feature of the environmental influence results from two-step mechanism of the carbene conversion (4). In this case the structural peculiarities of cages can effect both the kinetics of the hydrogen atom transfer and the RP reactions. The dynamics of these steps of one process can undergo the influence of local surroundings in different ways. Actually, the approaching to 0.3–0.4 nm of carbene and C—H bond is required for the hydrogen atom transfer. As a result of this step

the primary triplet RP is formed which can recombine only by the singlet state conversion. The frequency of singlet-triplet transforms in RP [13] is $10^8\,s^{-1}$. It is known that the small scales molecular motions connected with the rotational oscillations of small groups have frequencies of such order [14]. By this means the RP spin dynamics is in the same time scale with the molecular dynamics capable to provide transfers and minor turnings of radicals for recombination. At the same time the experimentally determined rate constants of the triplet carbene decay at 77 K in different organic matrices are very small [15] (10^{-3}–10^{-4}). In so doing the effective kinetic parameters have very low values of $E \cong 12$ kJ/mol and $\lg k_0 = 5.4$. Such values of Arrhenius parameters are markers of tunnel transfer of the hydrogen atom [16].

It must be emphasised that there are principal distinctions between RP resulting as active intermediates during the carbene decay and RP stabilized in organic glasses [17] and polymers [18] registered by the ESR characteristic spectra. The first type presents short-lived RP with the life time in cage compared with the spin evolution time ($\cong 10^{-8}$ s). The high recombination rate of such RP is conditioned probably by two reasons: the small distance between radicals (0.3 nm) and the time delay of the chemical bond rearrangements relative to the hydrogen atom transfer [19]. RP of second type is compared with isolated free radicals by their thermal stability. For them the distances between radicals are 0.5–0.8 nm. Their formation in the carbene reactions can be connected with molecular relaxation of the first type RP.

Thus, the reactions in the ground triplet state are typical by mechanism (4) for carbenes in glasses. In some systems this peculiarity can be explained in context of the singlet-triplet equilibrium (5) and the increase of population of the carbene triplet state at low temperatures. A number of literature data can be explained by the action of the space-orientation and molecular-dynamic factors of the nearest cage surroundings.

KINETICS OF THE LOW-TEMPERATURE CARBENE DECAY IN POLYMERS

The experiments were performed on carbenes of two types: DPC and cyclohexadienone carbene (CHC) as well as its 2,6-di-t-butylsub-

stituted analogue (DTBCHC). As precursors of DPC, CHC and DTBCHC diphenyldiazomethane (DDM), quinonediazide (QDA) and 2,6-di-t-butylquinonediazide (DTBQDA) were used. The kinetics of the carbene decay was studied in glass polymers and oligomer: polymethylmethacrylate (PMMA, $M_w = 124000$), fully deuterated PMMA (PMMA-D_s, $M_w = 230000$) polystyrene (PS, $M_w = 300000$), (PS-D_s, $M_w = 300000$), acetylcellulose (AC, $M_w = 330000$), oligopiperylene (OP, $M_w = 1200$). The concentrations of DDM, QDA, DTBQDA in polymer films accounted for about 10^{-3} mol/kg. QDA and DDM were added in PMMA, PS, AC from solutions in CH_2Cl_2 and in OP from the diethylether solution. All polymer and oligomer samples placed in tubes at a pressure of 10^{-4} torr. The samples were irradiated by filtered light of the mercury lamp at 77 K until the complete decomposition of diazocompounds was achieved. The photolysis of DDM in polymers was carried out by light with $\lambda > 500$ nm at 77 K. CHC and DTBCHC were generated by light with $\lambda > 300$ nm at 77 K. Kinetics of the carbenes decay was measured by signals of ESR spectra at 110G for DPC and 4600G for CHC (DTBCHC).

a. The Non-Exponential Kinetics of the Triplet Carbene Decay

The series of works concerning the low-temperature carbene decay was carried out in glass and polycrystalline solids [12, 20, 21]. In any single case the non-exponential kinetics was observed which can be described well by equation

$$N(t) = N_0 \exp(-Bt^{0.5}) \tag{6}$$

where B is the temperature-dependent parameter. The kinetic curves of the CHC decay in PMMA at 77–160 K are shown in Figure 1 [22]. The kinetic analysis of reactions, controlled by equation (6), was developed in detail [23]. The explanation of non-exponential kinetics is made taking account of the spread in the rate constants. In general case the time dependence of the particle concentrations is

$$N(t) = N_0 \int \rho(k) \exp(-kt) dk \tag{7}$$

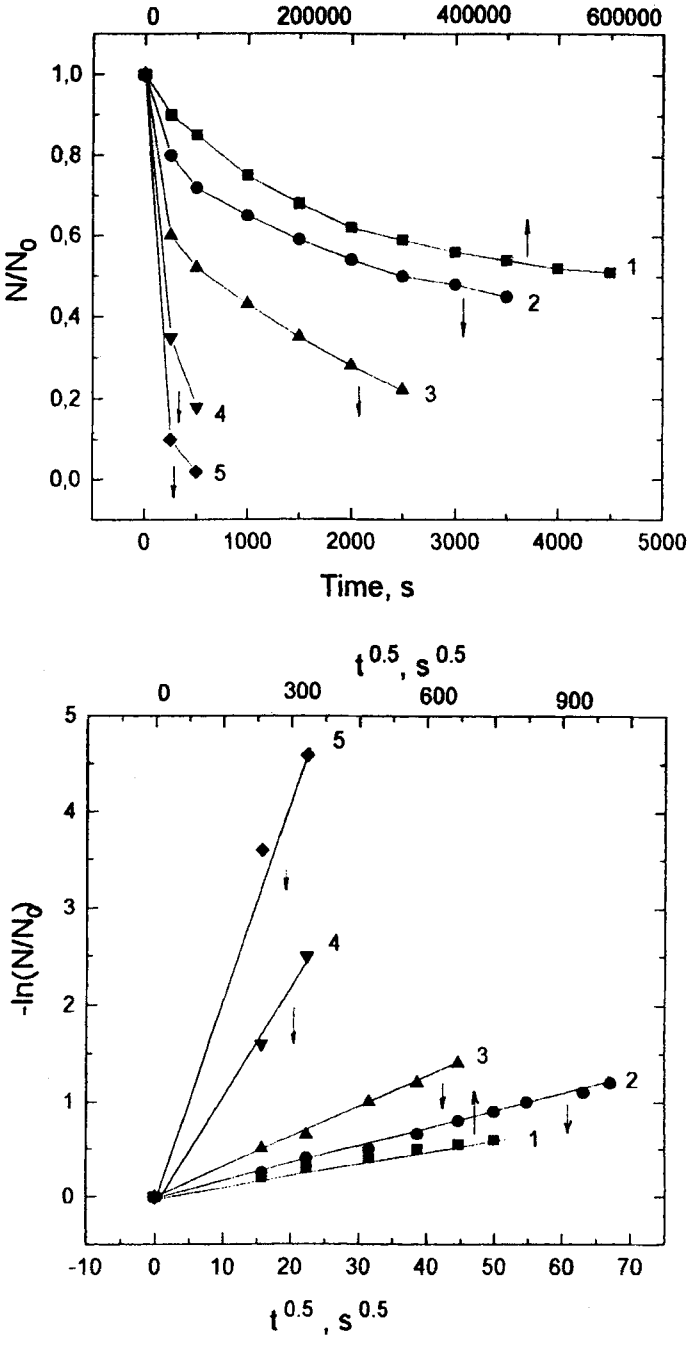

FIGURE 1 Kinetics of CHC decay in PMMA (a) and straightenings (b) in co-ordinates of (6): 1–77 K, 2–113 K, 3–128 K, 4–148 K, 5–161 K.

where $\rho(k)$ is distribution of the rate constants. The function

$$\rho(k) = \frac{b}{k^{1.5}} \exp\left(\frac{b^2}{4k}\right) \tag{8}$$

satisfy the equation (6). This function has extreme at $k = b^2/6$ that is the most probable value of the rate constant.

The other pattern appears when decays of DPC and DTBCHC proceed in PMMA [24,25]. The equation (6) does not work well in the wide temperature range of 77–183 K but the kinetic curves are straightened in co-ordinates $N/N_0 - \ln t$ (Fig. 2). Such description is characteristic of processes with so-called kinetic stop [26]. In this case the distribution function is evaluated by the following equation

$$\rho(k) = \frac{1}{k \ln(k_{max}/k_{min})} \tag{9}$$

where k_{max}, k_{min} are limiting values of the rate constants. The function $\rho(k)$ (9) is consistent with the wide spread of particles by their reactivity,

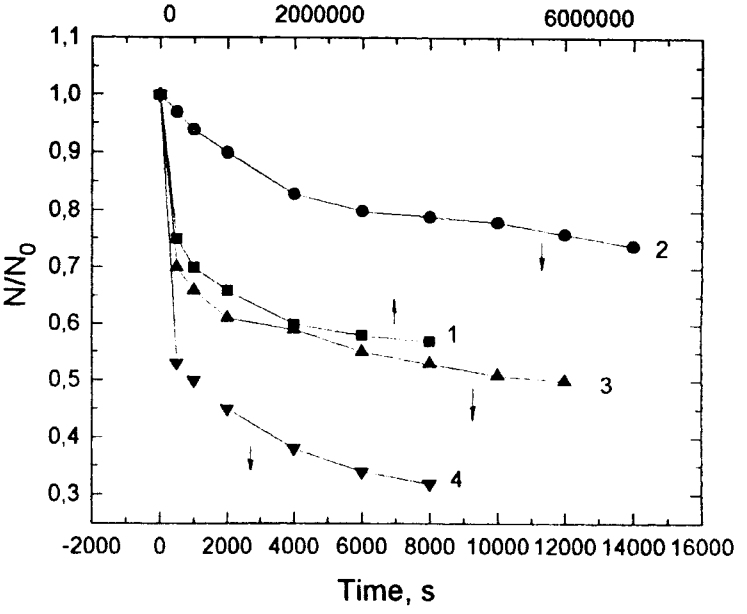

a)

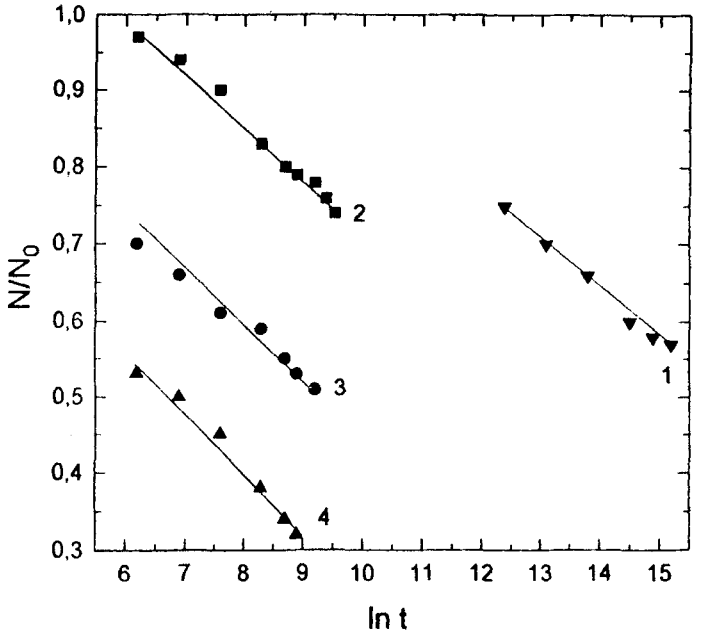

b)

FIGURE 2 Kinetics of DTBCHC decay in PMMA (a) and straightenings (b): 1–77 K, 2–100 K, 3–115 K, 4–131 K.

such as $\ln(k_{max}/k_{min}) = 13$ for DPC in PMMA at 77 K. The kinetic relationship for (9) is

$$\frac{N}{N_0} = \frac{-\ln k_{min} t}{\ln(k_{max}/k_{min})} \tag{10}$$

It should be noted that the function (8) is approximated easily by (9) when $k > k'$. This approximation is quite realistic for the narrow distribution of the rate constant: $\ln(k_{max}/k_{min}) < 10$. The K value is in agreement with k_{min}. The value of k_{max} can be evaluated from initial rates of the carbene decay. In this manner the values of k_{min} and k_{max} for kinetics presented by equation (6) can be estimated thanks to the closeness of (8) and (9) for narrow distribution.

The definite influence of space-orientation factors on the kinetic nonequivalence of triplet carbenes follows from the comparison of CHC and DTBCHC reactivities in PMMA. The width of distribution

of the rate constants of CHC decay $\ln(k_{max}/k_{min})$ turned out to be 5 at 77 K. In the same conditions $\ln(k_{max}/k_{min})$ of DTBCHC is 13. Apparently the volume of tert-butyl groups are responsible for large variety of the carbene centre and C—H bond orientations.

b. The Temperature Dependence of the Carbene Decay Rates in Polymers

The temperature dependencies of the rate constants during the carbene decay in polymers show appreciable deviations from Arrhenius law (Fig. 3). The effective activation energy drops from 12–16 to 5 kJ/mol with the temperature decrease from 180 to 77 K [22,24,25,27,28]. As observed, the kinetic peculiarities in polymers are co-ordinated with those of the hydrogen atom abstraction by free radicals in the course of tunneling. A number of works [29] indicated that the temperature dependencies can be straightened by the equation

$$k(T) = \alpha \exp(\beta T) \tag{11}$$

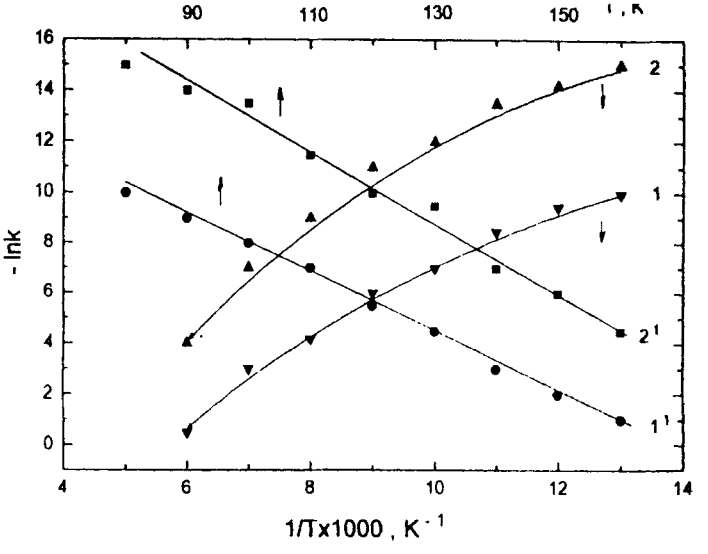

FIGURE 3 Temperature dependencies of k_{max}(1, 1') and k_{min}(2, 2') of CHC decay in PMMA.

where α and β are experimental constants. The equation (11) presents well the temperature dependence in polymers, as exhibited in Figure 3. It is important to note that $k(T)$ is in agreement with the tunneling of H atom by the reaction (4) for all numbers of triplet carbenes due to the likeness of k_{max} and k_{min} temperature plots. This result is essential to understand the cause of non-exponential kinetics. It is likely that the rate constant distribution is caused by the same scattering of parameters of the hydrogen atom tunneling.

There are two models to explain the exponential temperature dependence (11). One model accounts for this dependence by the thermal population of the highest oscillation levels of the hydrogen atom in potential well [29]. In this case the tunneling probability is increased in the atom transfer from higher levels as potential barrier becomes lower.

The another model is based on intermolecular oscillations close to the height and width of potential barrier [30]. It was shown that the excitation of the C—H bond highest levels can be neglected when the tunneling prevails over the atom transfer by activation. The bonding of hydrogenous type is assumed to arise between C—H bonds of the matrix molecules and radicals (or carbenes): $\equiv C—H^{\cdots}:C<$. Then the rate constant of the tunneling are expressible by the equation

$$k(T) = \omega_{C-H} W_0 \exp(\beta T) \tag{12}$$

where $\omega_{C\cdots H}$ is the oscillation frequency of C—H bond ($\omega_{C-H} \cong 3000\,cm^{-1}$), W_0 is the tunneling probability obtained by extrapolation of $k(T)$ at $T \to 0$

$$W_0 = \exp\left(-\frac{2}{\hbar} \int_{x_1}^{x_2} \{2m[U(x, A) - E]\}^{0.5} dx \right) \tag{13}$$

where m is the hydrogen atom mass, $U(x, A)$ is the potential energy. E is the hydrogen atom energy on the zero oscillation level, x_1 and x_2 are the potential barrier limits, A is the distance between carbene atoms in the complex of "carbene-molecule".

The estimation of U, x and the equilibrium A_0 was carried out at different temperatures [27]. The potential barrier was represented for

simplicity by the superpostion of two potential curves [31] of C—H bond of molecules and radicals resulting from the H atom transfer to carbenes

$$U(r, A_0) = -D\exp\left\{\left[-\frac{\gamma(r-r_0)^2}{2r}\right] + \exp\left[-\frac{\gamma(A_0-r-r_0)^2}{2(A_0-r)}\right]\right\} \quad (14)$$

In (14) r_0 is the C—H bond length, D is the dissociation energy of C—H bonds. This energy is assumed to be the same in molecules and radicals. The parameter γ is defined as follows

$$\gamma = \frac{m\omega_{C-H}^2 r_0}{D} \quad (15)$$

The probabilities of tunneling for given A_0 were estimated by equations (13–15) and these ones were compared with experimental W_0 [27]. In this manner A_0 values were determined. The Table I lists results obtained for DPC and CHC in OP. As it seen, the limit values of width and height are decreased with increasing temperature.

c. The Kinetic Isotope Effect on the Carbene Decay in Polymers

For the tunnel reactions the kinetic isotope effect (KIE) is expectd to exceed the one attributed to the difference between the oscillation zero energies of C—H and C—D bonds [32]. The literature data show,

TABLE I Parameters of hydrogen atom tunneling to CHC and DPC in OP

Carbene	*T, K*	U_{min}, *kJ mol*	U_{max}, *kJ/mol*	X_{min}, *nm*	X_{max}, *nm*	A_{0min}, *nm*	A_{0max}, *nm*
CHC	→0	150	208	0.115	0.140	0.375	0.400
	77	125	150	0.100	0.115	"	"
	133	108	121	0.094	0.100	"	"
DPC	→0	167	188	0.120	0.130	0.360	0.370
	77	138	159	0.110	0.118	"	"
	133	121	138	0.103	0.110	"	"

however, that this condition is not wet in low-molecular glasses. The kinetic analysis of DPC and DTBCHC decay in PMMA, PMMA-D_g and PS, PS-D_g has brought to light the characteristic properties of KIE. A complex relationship of KIE relative to the temperature and the degree of conversion was established. By way of example the kinetic curves of DTBCHC decay in PS and PS-D_g are shown in Figure 4 [25]. At higher temperatures the initial rates of decay in these polymers coincide but they are characteristically different at long-term conversion. It follows from these results that KIE depends on the triplet carbene reactivity. The ensembles of carbenes with higher rate constants are of smaller KIE at constant temperatures. KIE disappears practically at $T > 100-115$ K. The observed KIE was explained by H atom tunneling through oscillating barrier [33]. KIE was shown to fall off linearly in the temperature range

$$\frac{h\Omega}{4k} < T < \frac{hM\Omega^2}{m\Omega_{C-H}k}$$

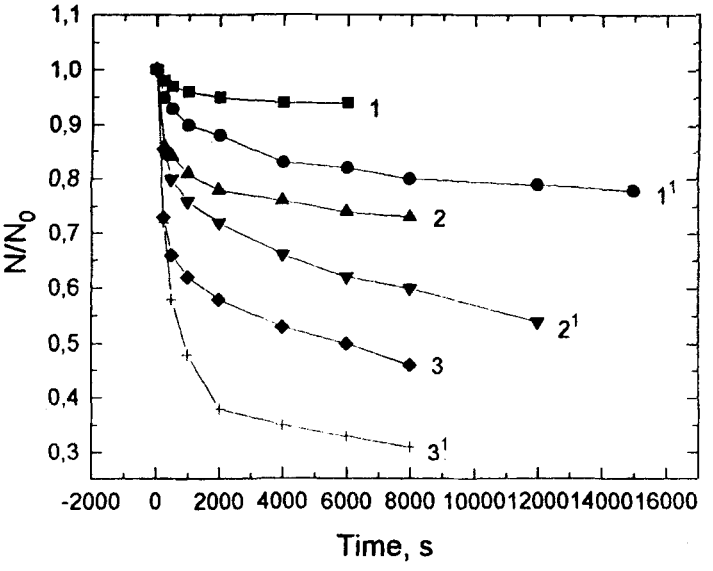

FIGURE 4 Kinetics of DTBCHC decay in PS and PS-D_s at 100 K–1, 1', 115' K–2, 2' and 136–3, 3'.

in accord with the equation (1c)

$$\ln\frac{k_H}{k_D}=\frac{\theta^{0.5}R_0^2}{2h}(m_D^{0.5}-m_H^{0.5})-\frac{\theta R_0^2}{2h}(m_D-m_H)\frac{kT}{hM\Omega^2} \qquad (16)$$

where $\theta = m_H\omega_{C-H}^2 = m_D\omega_{C-D}^2$ is the parameter characterizing the rigidity of C—H and C—D bonds, R_0 is spacing between potential wells, M is the effective mass of carbene-C—H bond complex, Ω is the intermolecular oscillation frequency in polymer matrix. At higher temperatures

$$T > \frac{hM\Omega^2}{m\omega_{C-H}} \quad \text{KIE varies as } T^{-2}$$

$$\ln\frac{k_H}{k_D}=\frac{h}{2\theta^{0.5}}\left(\frac{1}{m_H^{0.5}}-\frac{1}{m_D^{0.5}}\right)\left(\frac{M\Omega^2R_0}{kT}\right)^2 \qquad (17)$$

The analysis of KIE was carried out making use of equations (16) and (17). The temperature dependencies of $\ln(k_H/k_D)$ was plotted for different ensembles of carbenes defined by conversion degree $\psi = N/N_0$ at given temperature including the KIE of the maximal rate constants. These were found by extrapolation of straightening in co-ordinates ψ—$\ln t$ at $\psi \to 1$ [25]. The corresponding graphs for DTBCHC in PMMA and PMMA-D_g are shown in Figure 5. Two regions of the temperature plots can be resolved: the linear region from 77 to 100 K (Fig. 5a) and the region aligned in co-ordinates of equation (17) at $T > 100$ K (Fig. 5b). This behaviour of KIE enables us to form an estimation of the intermolecular oscillation frequency in PMMA activating the hydrogen atom transfer to triplet carbene. From the condition at which the linear relationship changed into the T^2 plot, the frequency was calculated as

$$\left(T=\frac{hM\Omega^2}{m\omega_{C-H}k}\right)$$

$\Omega = 52\,\text{cm}^{-1} = 10^{13}\,\text{s}^{-1}$. The value obtained correlates with Debye frequencies of molecular crystals [30].

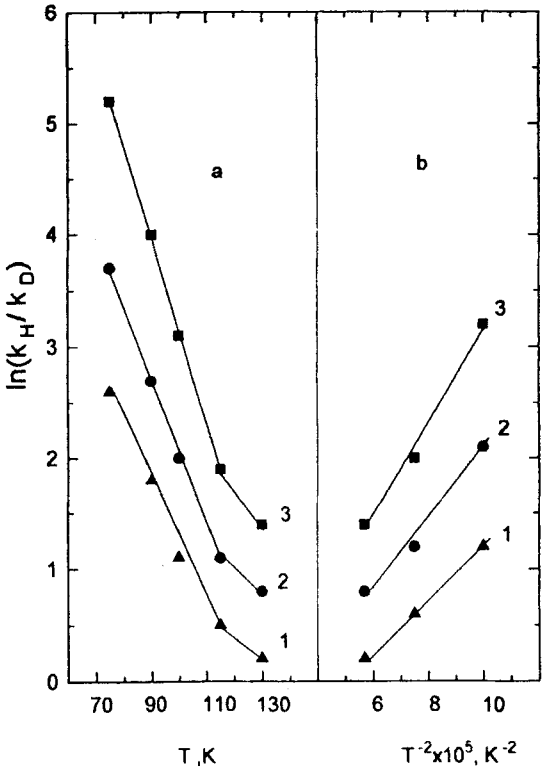

FIGURE 5 Temperature dependencies of KIE on DTBCHC decay in PMMA according to (16) (a) and (17) (b): $N/N_0 = 1(1), 0.8(2), 0.6(3)$.

The difference in distances between potential wells for transfer reactions of the carbene ensembles was determined through experimental temperature dependencies of KIE. It was interesting to compare this value and the rate constants of the carbene decay of the same kinetic ensembles. The results obtained are listed in Table II. As can be seen the decrease of the rate constant by an order is consistent with the increase of distance between potential wells of 0.006 nm. This fact confirms the tunnel mechanism of the hydrogen atom transfer [30].

d. The Magnetic Field Effect (MFE) on the Rate of the Carbene Decay in Low-molecular Glasses and Polymers

MFE is an important tool to study the mechanism of radical reactions. This research method can provide unique information about the

TABLE II The dependence of rate constants of DTBCHC and DPC decay in PMMA and PMMA-D_g on change of equilibrium distances in complex "carbene-C—H bond"

Carbene	*T*, K	ψ	$\Delta R_0 = R_0^{\psi} - R_0^{\psi=1}$, nm	$-lg\, k_H$	$-lg\, k_D$
DTBCHC	77	1.0	0	4.0	5.0
	100			2.7	3.3
	115			1.7	1.8
	131			0.6	0.6
	77	0.8	$6\ 10^{-3}$	5.0	6.4
	100			3.6	4.4
	115			2.6	2.9
	131			1.4	1.6
	77	0.6	$1.3\ 10^{-2}$	6.2	7.9
	100			4.6	5.6
	115			3.4	3.9
	131			2.3	2.6
DPC	77	1.0	0	4.0	4.9
	148			0.9	1.3
	183			−0.9	−0.9
	77	0.8	$1.2\ 10^{-2}$	5.0	6.3
	148			1.7	2.3
	183			0.4	0.5
	77	0.5	$2.7\ 10^{-2}$	6.7	8.6
	148			2.9	3.9
	183			1.3	1.6

nature of kinetic non-equivalence in the solid phase radical reactions owing to the determination of the cage structural-physical parameters.

The kinetic curves of DTBCHC decay in ethylacetate (EA) and hexaethylsiloxane (ES) in the magnetic field of different strength are shown in Figure 6 [34]. Since the highest degree of conversion had not exceeded 20% at 77 K, the initial rates (W_0) were chosen as experimental parameter undergoing the magnetic field influence. The dependencies obtained are given in Figure 7. It is seen that these rates are changed as a function of field with extremes in both glasses.

The rate is also affected by magnetic field in polymers (Fig. 8) [35]. In this case magnetic dependencies vary unmonotonically. The abrupt changes amounting to 40% in PMMA and 50% in AC take place within fairly narrow ranges of field (2000–3000 G). The fact of MFE on the triplet carbene decay at 77 K resulting from the hydrogen atom transfer as such, makes it possible to conclude that this process is

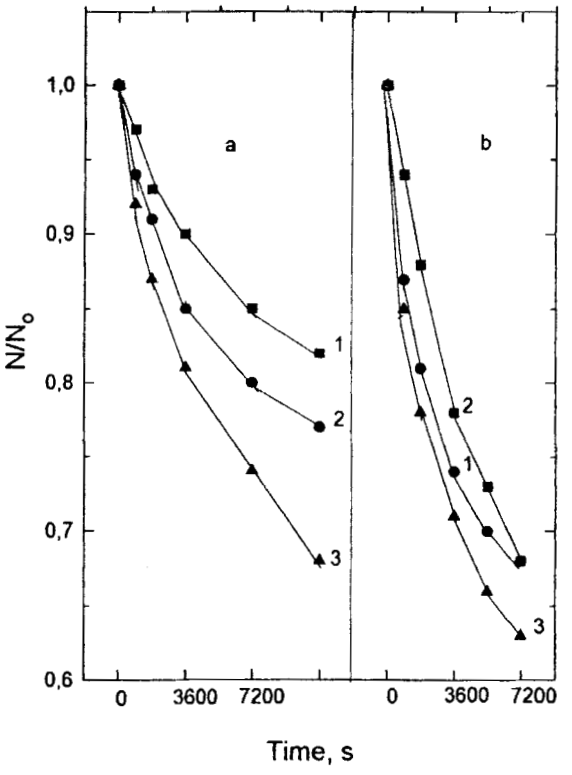

FIGURE 6 Kinetics of DTBCHC decay (77 K) at magnetic fields 1–0 mT, 2–300 mT, 3–160 mT in EA (a) and 1–0 mT, 2–300 mT, 3–30 mT in ES (b).

reversible. To explain MFE the following mechanism can be suggested

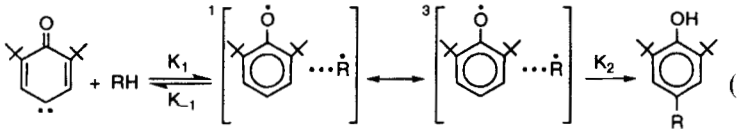

(18)

The triplet RP is formed in the primary act. This RP undergoes the singlet-triplet evolution. RP in the triplet state is converted into original triplet carbene by the back hydrogen atom transfer but in the singlet state RP is recombined. The efficiency of recombination is dependent on the relative population of triplet and singlet levels of RP (P_T/P_S). From (18) it follows that effective rate constants of DTBCHC

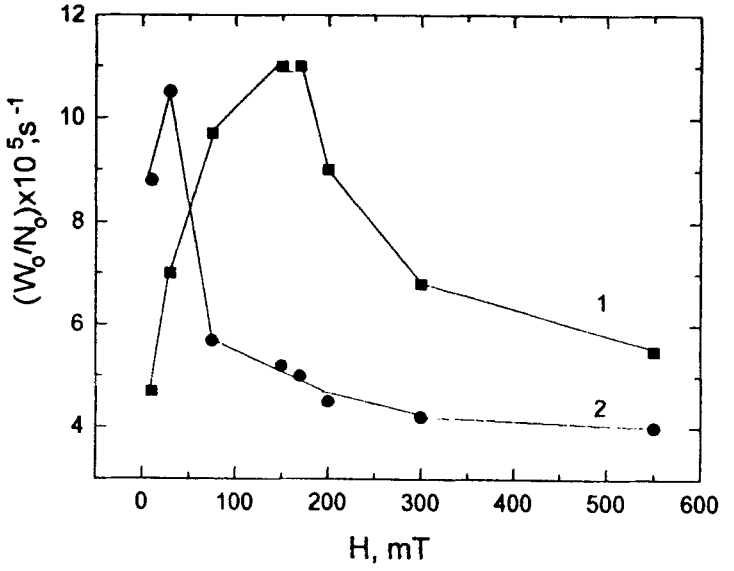

FIGURE 7 MFE on DTBCHC rate decay (77 K) in EA (1) and ES (2).

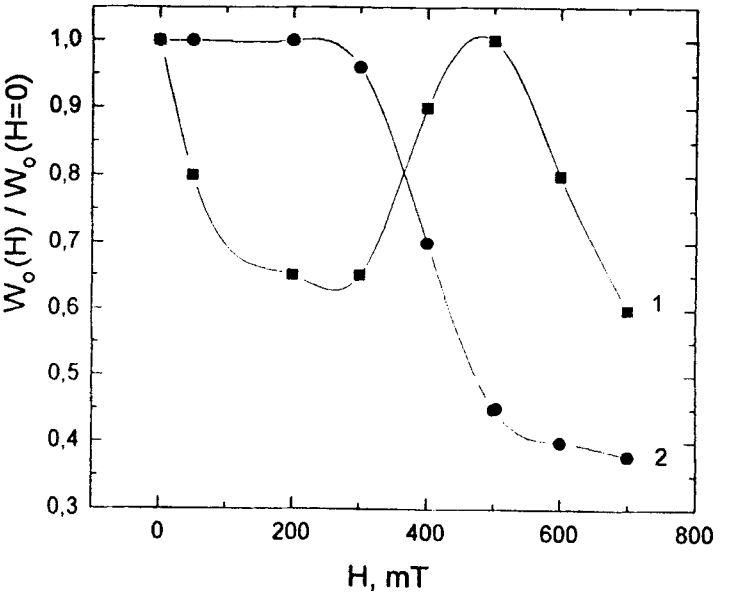

FIGURE 8 MFE on DTBCHC rate decay (77 K) in PMMA (1) and AC (2).

decay in zero field is expressed as

$$k_{ef} = \frac{k_1}{(k_{-1}P_T/k_2P_S) + 1} \tag{19}$$

It will be noted that k_{ef} at 77 K is about $10^4\,s^{-1}$ whereas characteristic time of spin dynamics is 10^{-8} s. For the MFE initiation k_2 and k_1 should be comparable to the spin evolution frequency. In this connection one can conclude that the limiting step of the low-temperature decay of carbenes is the formation of primary triplet RP. This stage defined by k_1 includes the cage reorganisation for favourable mutual orientations of C—H bonds and carbenes to create the tunnel transfer of H atom. The slow process of the cage reorganisation ($\approx 10^4$ s) seems to lie in the leveling of two potential wells in energy needed to occur the forward and the back atom tunneling. The fluctuation of the polarization forces as a result of the polar group motions can induce changes of the potential well configurations with lime. In so doing the two energy levels are varied and can coincide for a while with the subsequent atom transfer.

The magnetic field splits the triplet level of RP into three levels T_0, T_+ and T_- with the result that the probability of the triplet-singlet conversions is decreased. In sufficiently high field the mixture of T_0 and T_+ by the HFI mechanism may be neglected. Then the effective rate constant is averaged over the rate constants of RP arising in the primary act on all T_0, T_+ and T_- levels. The equation (19) is turned to $k_{ef} = k_1\varphi(\mathrm{H})$ where

$$\varphi(\mathrm{H}) = \frac{1}{3}\left[\frac{1}{(k_{-1}P_{T_0}/k_2P_S) + 1} + \frac{1}{(k_{-1}P_{T_+}/k_2P_S) + 1} + \frac{1}{(k_{-1}P_{T_-}/k_2P_S) + 1}\right] \tag{20}$$

In (20) the relative populations P_{T_+}/P_S and P_{T_-}/P_S are functions of magnetic field. On account of the Figure 6 plots MFE observed can be believed to result from the exchange interactions J of non-pair electrons in intermediate short-lived RP. The exchange interaction, splitting triplet and singlet levels of RP, can lower the probability of

the spin evolution in the zero field. Within some interval of magnetic field the mixture of T_- and S levels makes it possible to increase abruptly the population of the RP singlet level. As a consequence, the part of primary RP, disappearing in the triplet state by the back transfer of H atom with the formation of the starting carbene, is reduced and accordingly the fraction of RP decaying by the recombination is increased. Thus the rate of DTBCHC decay is built up to a maximum at the field strength complying with the resonance condition.

$$2J = -\frac{a}{8} \pm \frac{g\beta H}{h} \tag{21}$$

The question of the J significance in magnetic effects is dealt in literature in some detail [36]. It follows from available data that MFE with the dependence observed of kinetic constants on the field strength can occur under specific conditions. The exchange interaction as a function of distance takes usually the form of exponential law [37]. The average spacing in RP must be cosistent with J, exceeding by energy other interactions mixing S and T levels (spin-oribital, dipole-dipole, HFI). The lifetime of radicals in the field of the S and $T_\pm$ intersections must be sufficient for the intersystem crossing to occur. The low-temperature decay seems to fit these requirements. In such reactions small distance (≈ 0.35 nm) RPs are formed and the strong restriction of the molecular mobility increases essentially the lifetime of RP in certain configurations (to 10^{-7}–10^{-8} s).

All points of experimental plots (Fig. 6) were obtained under conditions when the theory of the RP spin dynamics in high magnetic fields may be used to analyse MFE. It should be pointed out the equation (20) was derived, assuming that triplet RPs are formed equally probably in T_0, T_+ and T_- without transitions between triplet levels. Consequently the different channels of singlet-triplet transitions are displayed in the additive manner.

The complete analysis of MFE was accomplished for RP with one magnetic nucleus of 1/2 spin. The approximations can be applied for a more complex case when RP contains several protons. Then the root-mean-square constant of HFI with all protons may be introduced into the treatment:

$a = (\Sigma a_{1k}^2 + \Sigma a_{2n}^2)^{0.5}$, a_{1k} and a_{2n} are HFI constants of RP. The Kaptein's model [38], in which the radical distances are fixed, was used to deal with the spin evolution of RP. By this model the singlet state population of RP is deduced

$$P_{S(T_0)} = \frac{a^2\tau^2/8}{1 + (a^2/4 + 4J^2)\tau^2} \tag{22}$$

$$P_{S(T_\pm)} = \frac{a^2\tau^2/4}{1 + [a^2/2 + (2J + a/4 \pm g\beta H/4)^2]\tau^2} \tag{23}$$

where τ is the lifetime of RP, a is HFI, RP is formed in primary act in T_0, T_+ and T_-. The relative populations of singlet and triplet levels in magnetic field $P_T/P_S = (1 - P_S)/P_S$ are estimated by (22) and (23). In all studied systems the HFI effective constant amount to 30–40 G ($5.2–6.9\ 10^8$ rad/s). If $\tau \approx 10^{-8}$ s and $a^2\tau^2 \gg 1$ then

$$\frac{P_{T_0}}{P_S} \approx \frac{8}{a^2}(2J)^2 + 1 \tag{24}$$

$$\frac{P_{T_\pm}}{P_S} \approx \frac{4}{a^2}(2J + a/4 \pm g\beta H/h)^2 + 1 \tag{25}$$

The dependencies of probabilities of the RP recombination on magnetic field can be plotted by relations (20, 24, 25) [35]. The form of $\varphi(H)$ is determined by J and k_{-1}/k_2 (Fig. 9). At J comparable to the effective HFI constants $\varphi(H)$ decreases steadily to a pleateau while $\varphi(H = 0) \approx 3\varphi(H_\infty)$ in accordance with numbers of the intersystem crossing channels working effectively in the zero and high magnetic fields. The dependence has a maximum at $H = (2Jh)/g\beta)$.

The comparison of estimated plots of Figure 9 with the experimental ones shows that MFE observed in PMMA and AC is approximated by the set of $\varphi(H)$ with different values of J. So in PMMA two types of BR can be resolved with $J = 0$ and $J = 4.4\ 10^{10}$ rad/s. The availability five types of RP with $J = 0$; 0.87; 1.7; 2.62; $3.50\ 10^{10}$ rad/s can account for MFE in AC.

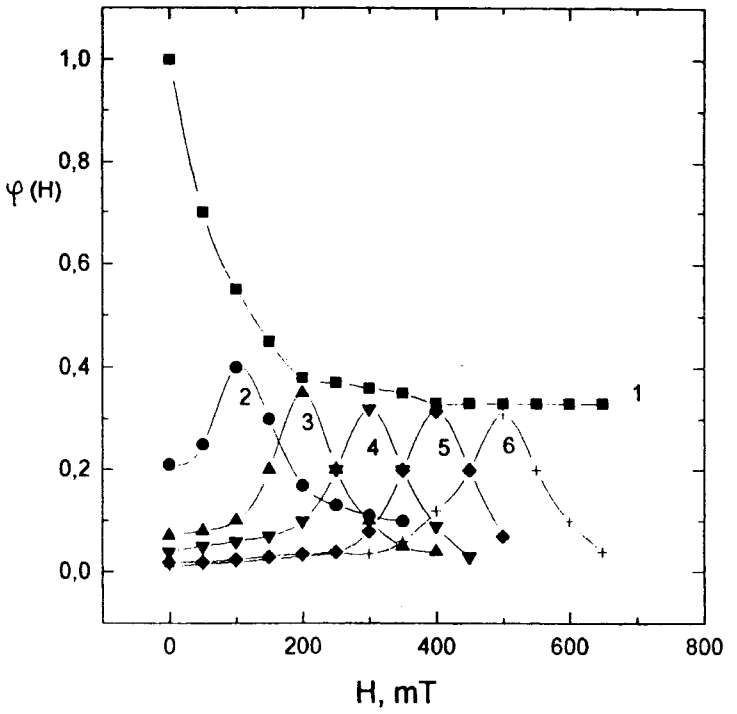

FIGURE 9 Probabilities of RP recombination in magnetic field at $2J = 0$ (1), $1.7\ 10^{10}$ (2), $3.5\ 10^{10}$ (3), $5.2\ 10^{10}$ (4), $7.10\ 10^{10}$ (5), $8.8\ 10^{10}$ rad/sec (6); $k_{-1}/k_2 = 1.8\ 10^{-3}$.

The distribution of J corresponding to the MFE scale cannot be due to the spacing of radicals. The fact is that calculations [36] using $J = J_0 e(-\sigma r)$ must give Δr of the order of 0.05 nm for the J distribution in AC. At 77 K the increase of equilibrium distances in the complex of carbene-C—H bond by 0.006 nm gives rise to the tenfold decrease of the rate constant of DTBCHC decay (Tab. II) whereas the magnetic field affects the rate by 40–50%. The orientation factor, connected with angles of rotation of the orbital axes of non-pair electrons about one another, seems to be responsible for the exchange energy spread.

For example, calculations performed for the model RP39 show the change in J to a primarily affected by the angles of rotation.

The results obtained show that MFE at cryogenic temperatures is qualitatively similar to that the solid phase. The degree of distinctions is defined by the nature of matrix. The reaction cages are more homogeneous relative to J in low-molecular glasses of EA and ES as

compared with polymers in view of pronounced changes of rates in magnetic field.

THE MECHANISM OF THE CARBENE REACTION PRODUCT FORMATION IN POLYMERS

There is a need to study both the ultimate molecular products and the intermediate radicals to establish the carbene reaction mechanism in polymers. But, in spite of the wide use of the different spectral techniques (UV, IR, ESR) and the flash photolysis to determine such characteristics of carbenes as the geometrical parameters, the oscillation frequencies, the electron transitions, the products of the primary reaction of carbenes with the environment and poorly known. The data about the free radical products with the low-molecular organic solids are reported only in a few works [40–43].

a. The Structure of RP Resulting by the Low Temperature Reactions of CHC and DPC in Polymers

The ESR spectra of the insulated triplet CHC [44] and the spectrum at $g \approx 2$ were observed at 77 K in the PMMA films with QDA during irradiation by light. The spectrum shown in Figure 10a was obtained under action of the light with $\lambda > 380$ nm [22]. It is the characteristic signal of RP [17]. The average distance (r) between radicals in RP can be determined from parameters of dipole–dipole interaction $D_{\perp} = 114$ G, $D_{II} = 228$ G by the equation

$$D_{\perp} = \frac{27.8}{r^3} \tag{26}$$

The estimation gives the value of $r = 0.6$ nm. The signals of isolated radicals are obsrved in the central region of spectrum. It was established that the RP and isolated radical proportion in PMMA is about 10% of triplet CHC, and therefore, this value does not change during QDA photolysis. From this fact it transpires that all three products of the QDA photolysis at 77K are formed in parallel. The thermal decay of the stabilized triplet CHC in a time of irradiation can be ignored, that is, the

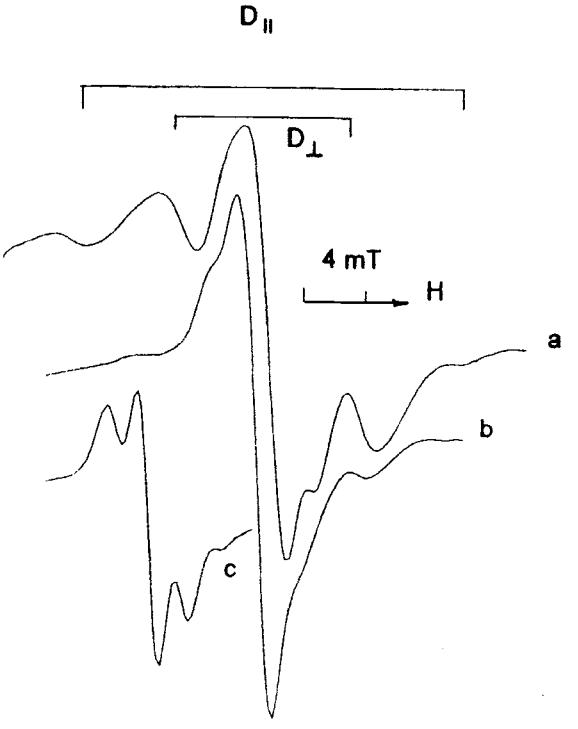

FIGURE 10 ESR spectra of PMMA with QDA irradiated at 77 K by light $\lambda > 380$ nm (a), $\lambda > 300$ nm (b) and after heating of (a) at 183 K. (c).

thermal reaction of carbenes with PMMA cannot give the PR and radical formation with detectable rate. The effect observed is explained by the excess of the absorbed energy of 200 KJ/mol in comparison with the dissociation energy of the quinonediazide C—N bonds. The concentration of the excess energy in cages leads to the essential increase of the carbene reaction rate with C—H bonds of macromolecules.

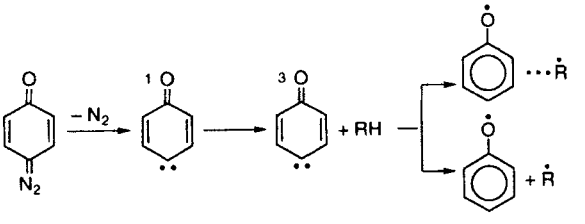

(27)

The main part of triplet CHC ($\approx 90\%$) is stablised at 77K as a result of this energy dissipation in the polymer matrix. The phenoxy radical formation by the reaction (27) is exhibited by UV spectrum. It contains the bands with maximum at 390 nm and 405 nm [45].

The absence of the thin structure in ESR spectrum (Fig. 10a) does not permit immediately to establish the nature of PMMA radicals involved in RP. To identify these radicals the typical reactions of thermal and photochemical conversions [46, 47] were used. The signal of RP in ESR spectrum disappears during the shorter wave light irradiation ($\lambda > 300$ nm Fig. 10b). The PMMA macroradicals sensitive to the light with $\lambda > 300$ nm have the structure $\sim CH_2C(CH_3)(COO\dot{C}H_2)CH_2\sim$ (I). These radicals are decomposed in following manner

$$\sim CH_2C(CH_3)(COO\dot{C}H_2)CH_2\sim \xrightarrow{h\nu} \sim CH_2\dot{C}(CH_3)$$

$$CH_2\sim (II) + CO + CH_2O \qquad (28)$$

$$\lambda > 300 \text{ nm}$$

As a result of the macroradical photodissociation the distance between the unpair electrons in RP must increase by at least 0.3 nm and RPs are transformed into isolated radicals.

The radicals II dissociate with the breaking of macrochain.

$$\sim CH_2\dot{C}(CH_3)CH_2\sim \rightarrow \sim CH_2\dot{C}(CH_3)(COOCH_3)\,(III)$$

$$+ \sim CH_2C(CH_3)(COOCH_3)CH_2\sim \qquad (29)$$

Actually, the nine components ESR spectrum, belonging to radicals (III), was observed by the sample heating to the room temperature. The ESR spectrum of radicals (I) was detected at 183 K in pure form (Fig. 10c). By this mean RPs and isolated radicals are formed at 77K by the hydrogen atom abstraction from the PMMA ester groups.

The ESR spectrum in the $g \approx 2$ region, shown in Figure 11, was observed during the irradiation of OP with QDA by light with

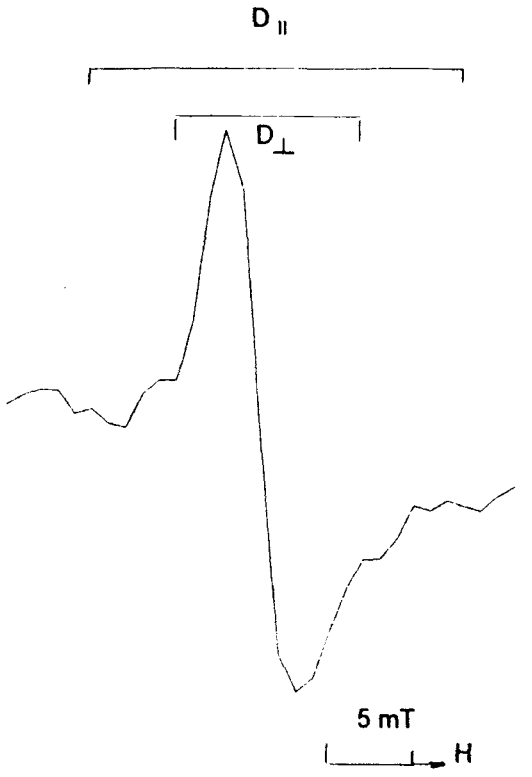

FIGURE 11 ESR spectrum of OP with QDA irradiated by light $\lambda > 370$ nm at 77 K.

$\lambda > 370$ nm among the signal of triplet CHC [27]. This spectrum involves the unresolved central component at brims of which further components are seen. From the spectrum shape analysis it follows that the photodecomposition of QDA in OP at 77K brings into existence isolated radicals and RP in the ratio of 3:2. The values of splitting in the zero field $D_{\perp} = 100$G and $D_{II} = 200$G show that the average distance between unpair electrons is 0.64 nm. The process going on at low temperature irradiation of QDA in OP can be represented by scheme similarly to (27). For lack of a rather resolved ESR spectrum the nature of the OP radicals constituent of RP along with phenoxy radicals can be established by the circumstantial evidence obtained in the spectral investigation [48]. The macroradicals of OP are formed as a result of the hydrogen atom transfer to carbenes from allylic C—H bonds of 1.4 and 1.2 links. Based on the ESR data it was concluded

that in RP allylic radicals $\sim CH_2CH{=}CHC(CH_3)CH_2\sim$ (IV) and $\sim CH_2C(CH{=}CHCH_3)CH_2\sim$ (V) are present.

The several kinds of paramagnetic particles are formed in samples of OP with DDM irradiated at 77K by light with $\lambda > 500$ nm. The triplet DPC is identified by the characteristic ESR spectrum [49] and also by the absorbance band at 465 nm in UV spectrum [50]. Hand in hand with the appearance of ^{3}DPC signal the ESR spectrum with $g \approx 2$ is registered (Fig. 12a). The anisotropic doublet signal of triplet RP with poor resolution is observed. In this system OP macroradicals and diphenylmethyl radicals Ph_2CH(VI) can be formed. The dipole–dipole interaction of unpair electrons in RP is characterised by

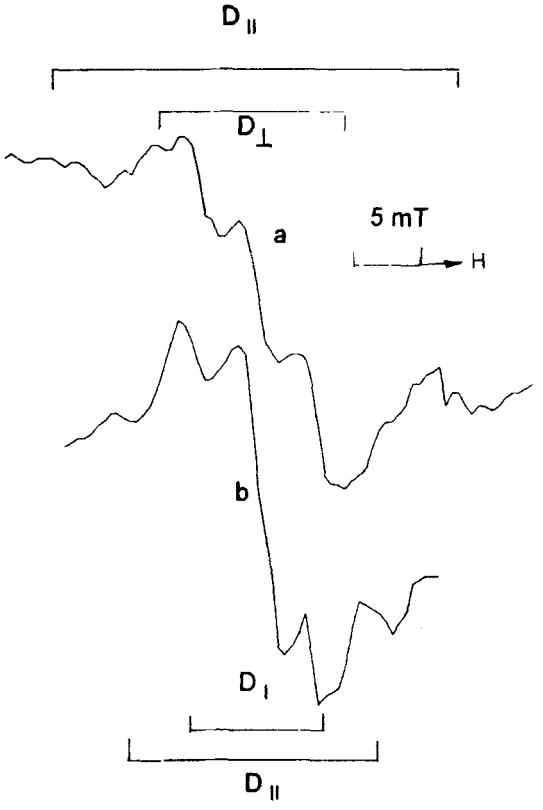

FIGURE 12 ESR spectra of OP with DDM irradiated by light $\lambda > 500$ nm at 77 K (a) and after heating of (a) at 145 K (b).

$D_{\perp} = 195$G and $D_{II} = 390$G. These values show that the average distance between electrons in such pairs is 0.52 nm that is significantly less than in RP discussed above in PMMA and OP with CHC. In spite of the poor resolution the splitting of 10–15G typical of radicals (IV), (V), (VI) can be observed. The heating of samples leads to the RP spectrum change (Fig. 12b). The initial signal with $D_{\perp} = 195$G disappears and the signal with $D_{\perp} = 110$G remains which corresponds to RP with the average distance between radicals of 0.63 nm. In addition the severe narrowing of the spectrum components from 70 to 15G takes place.

b. Kinetics of the Biradical Formation by the Low Temperature Conversions of DPC in Polymers

The formation of new biradical (BR) product in OP indicates some distinctive features of the triplet DPC reactions in comparison with CHC. To establish the BR nature and the formation mechanism the DPC conversions in different polymers were studied. The appearance of identical ESR spectrum was discovered for DPC by photolysis of DDM in PMMA, PS, PMMA-D_8, PS-D_8 and polycarbonate (PC) [51, 52]. One can assert that they are not RP because of the same parameters of ESR spectra characterising distances between radicals.

Low molecular substances are present mostly in defects of polymer packing [53]. Therefore, one can suppose that carbenes are accumulated both in isolated states and in clusters of two or more DPC in such low density domains. Therefore the carbene dimer conversion products can be presented as follows

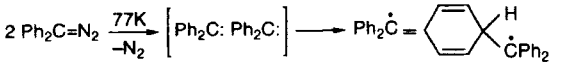

(29)

The reaction of carbenes localized in micropores is interesting in two aspects. The BR yield must reflect apparently the non-homogeneity of DDM distribution and can be used to estimate the distribution by concentrations of other low-molecular additives in solid polymers. The kinetics of this process must depend on the intensity of small-scale molecular mobility of the micropore surrounding. The BR

formation by the reaction (29) is confirmed by the increase of their yields, determined by the ratio of initial rates of the BR and isolated DPC formation, with the DDM concentration increase (Fig. 13).

The dependence of BR yield on DDM concentration is described satisfactorily by the empirical equation

$$\mu = \frac{\mu_\infty [\mathrm{DDM}]}{C + [\mathrm{DDM}]} \tag{30}$$

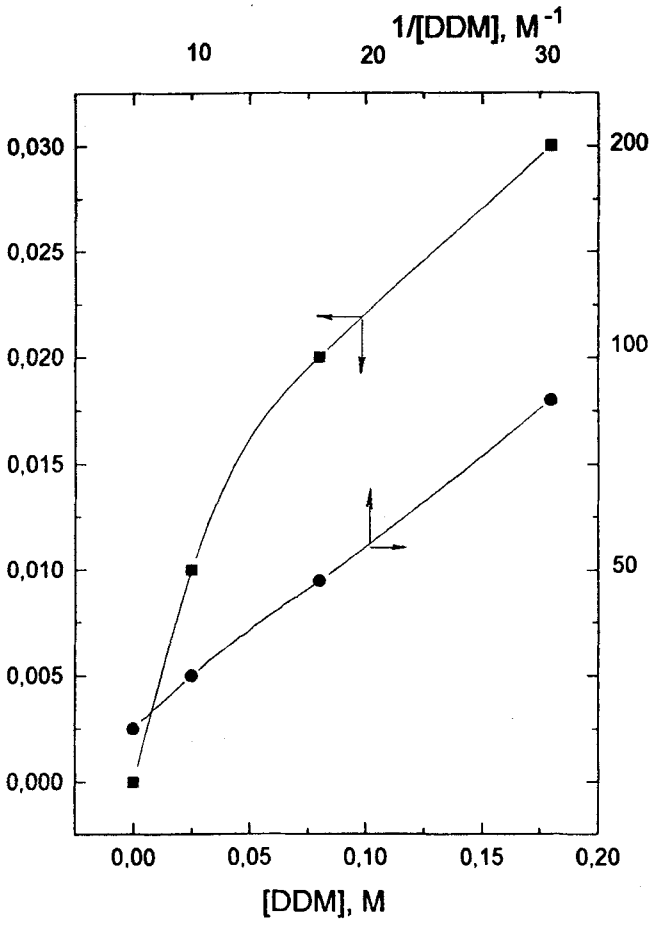

FIGURE 13 The dependence of BR yield in PC on DDM concentration.

where μ_γ and C are empirical constants. The deviation of μ([DDm]) from linearity is connected evidently with the high filling of polymer micropores at [DDM] > C. The intense line belonging to BRs with distances between spins of 0.9–1.0 nm and more is appeared at the centre ESR spectrum at deep stages of DDM photolysis. Such particles are formed if three DPC will react

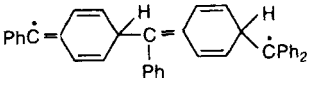

These BRs are produced in bigger clusters. The EST spectrum shows that the portion of 'polymeric' BR in PC and PMMA does not exceed 20% relatively to the entire current of BR.

The results obtained can be used to evaluate the non-homogeneity of low molecular additives similar in to DDM chemical structure. For example, the analogous distribution of biomolecular, three molecular and polymolecular clusters of some photostabilisers, antioxidants, photosensibilisers (salicylates, benzophenones, bisphenols) must also exist in glass polymers.

The peculiarities of the BR formation in the course of thermal reaction are expressed by the annealing of samples irradiated at 77K shown in Figure 14. These curves were obtained by exposing the samples to isothermal conditions. The annealing curves are displaced relatively to one over the another at 15–20K showing that the reactivity of carbenes in clusters depends on the nature of polymer. It was established that annealing curves may be considered as the characteristics of the distribution of the particle reactivity [26]. The kinetics of the BR formation in PC is shown in Figure 15. These kinetics are straightened in coordinates of "concentration–lg t". This fact suggests that the distribution function of carbenes has the straight-angle type [26] by the activation energy of the BR formation

$$\rho(\mathrm{E}) = \frac{1}{E_{\max} - E_{\min}}, \quad E_{\min} < E < E_{\max} \tag{31}$$

The gradual annealing of mobility of the kinetic nonequivalent carbenes in clusters determines the temperature dependence of the BR

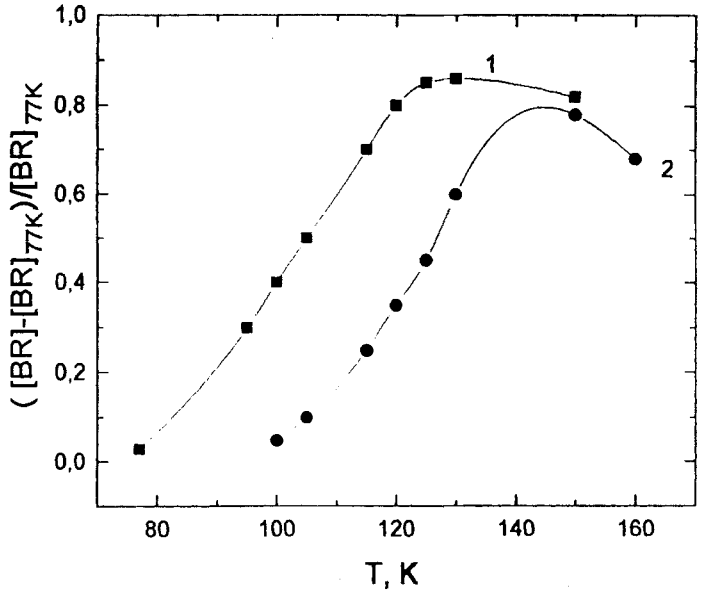

FIGURE 14 Annealing curves for BR formation in PC (1) and PMMA (2); the exposure time is 4 min in isothermal conditions.

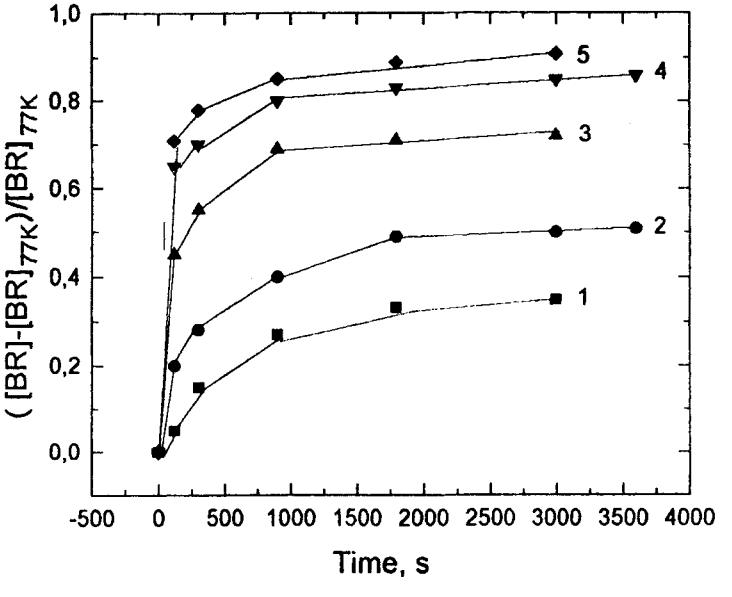

FIGURE 15 Kinetics of BR formation in PC at 1–94 K, 2–100 K, 3–107 K, 4–115 K, 5–120 K.

formation rate. The rate constant dispersion in PC permits to define the Arrhenius parameter distribution which in general case is connected with distributions of both the activation energy and the pre-exponential factor. The method stated in work [54] may be used to determine the distribution of these parameters. The kinetic curves set $\theta(t, T)$ (Fig. 15) was cut by horizontal straight lines and the values of the rate constants $k(\theta, T) = t^{-1}$ (θ, T), determining the reactivity of given kinetic ensembles, were found. Then the temperature dependencies of $k(\theta, T)$ values were constructed in Arrhenius co-ordinates and activation energies and pre-exponents were determined. The $\theta(E)$ and $\theta(k_o)$ plots are the distribution integral functions of the corresponding parameters. These plots are essentially linear (Fig. 16) and the distribution functions of carbenes in clusters of Arrhenius parameters may be considered to be of a straight angle type. The

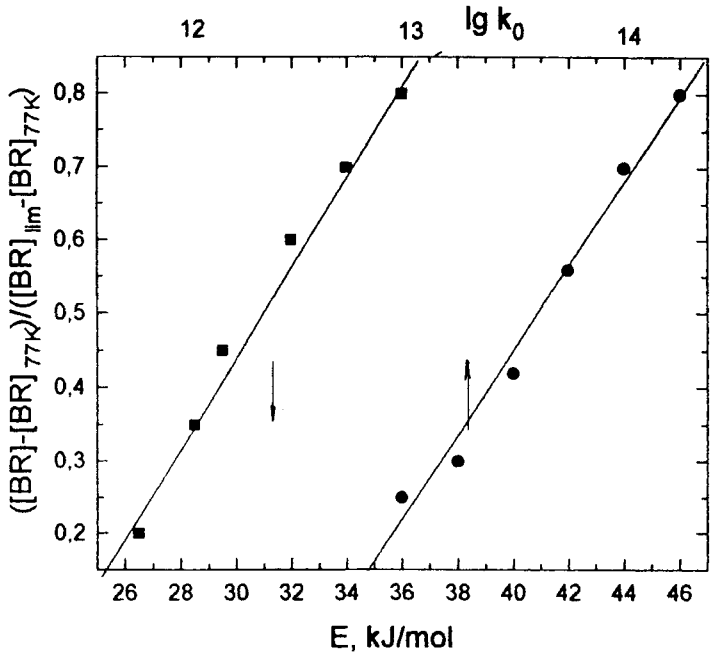

FIGURE 16 Distribution functions of DPC by Arrhenius parameters of BR formation in PC.

extrapolation of linear relationships of $\theta(E, k_o)$ to 1 and 0 gives the values of E_{max}, E_{min}, $\lg k_{0\,max}$ and $\lg k_{0\,min}$. These values in PC are $E_{max} = 38$ kJ/mol, $E_{min} = 26$ kJ/mol, $\lg k_{0max} = 14.4, \lg k_{0\,min} = 12.8$.

The activation energy values obtained are typical of the relaxation processes in PC (40 kJ/mol) caused by the motions of monomer links and side groups of macrochains. These values are adjusted with the activation energy of the spin probe rotation [55, 56]. The reaction of the BR formation in PC is controlled by rotary motions of carbenes. In fact, the values of $k_0 = 10^{13} - 10^{14}$ s^{-1} are compared with the frequencies of the orientational motions of the low molecular particles in polymers. One can note the small dispersion of the Arrhenius parameters: $\Delta \lg k_0 = 1.6$, $\Delta E = 12$ kJ/mol.

In PMMA the limiting values are $E_{max} = 50$ kJ/mol, $E_{min} = 22$ kJ/mol, $\lg k_{0\,max} = 16.0$, $\lg k_{0\,min} = 10.5$. The average Arrhenius parameters of the BR formation are $\lg k_{0\,av} = 13.25$, $E_{av} = 36$ kJ/mol. These values correlate satisfactorily with the activation energy and the rotation time of spin probes in PMMA: $E = 38$–42 kJ/mol, $\lg \tau = -13.2$ [55]. But the high dispersion of Arrhenius parameters attracts attention: $\lg k_0 = 6.5$, $E = 28$ kJ/mol.

The results obtained may be explained by the existence of wider scattering of hindered molecular motions in PMMA that are annealed with the temperature increase. The calculations [57] shows that the activation energy of the side ester group rotations combined with relative vibrations of a main chain near equilibrium positions is 21.6 kJ/mol. This value coincides with the minimum activation energy for the BR formation. But the activation barrier of the ester group rotation is increased with the decrease of rotational angles from the equilibrium values. The calculation gives maximum potential barrier of 68 kJ/mol for torsional oscillations around the C—C bonds of a main chain. Therefore, the increase of activation energy to 50 kJ/mol can be considered as the transition of the carbene orientational dynamics into regime controlled mainly by the macrochain mobility. In this manner the differences observed in kinetic regularities of the BR formation for two polymers are caused by molecular organisation of environments. In the temperature region studied the distribution width of the rate constants determined by $\lg(k_{max}/k_{min})$ is 1.5–2 times wider in PMMA than in PC. On the basis of the rate constant dispersion one can conclude that the structural

non-homogeneity of the micropore surrounding in PMMA is higher as compared with PC.

The BR thermal decay prevails at $T > 130$–150 K over their formation (Fig. 14). The kinetics of the BR decay expresses molecular dynamics defining the reaction rate for bigger particles relative to carbenes. The kinetic data show that BRs are unequal in the reaction of decay too. The kinetic curves of this process in PMMA are straightened in co-ordinates $[BR]/[BR]_0 - \lg t$ at 183–218 K (Fig. 17). One can see that the slope angle of plots does not change with the temperature, therefore the BR non-equivalence observed in a given temperature interval does not correlate with the activation energy distribution. The rate dependence of the BR decay follows the Arrhenius law. The limiting constants are $k_{max} = 5\ 10^{12} \exp(-46 \pm 4$ kJ/RT) s^{-1}, $k_{min} = 10^9 \exp(-46 \pm 4$ kJ/RT) s^{-1}. It is followed from limiting values that in PMMA the activation energy of the BR decay corresponds to the maximum activation energy of the BR formation.

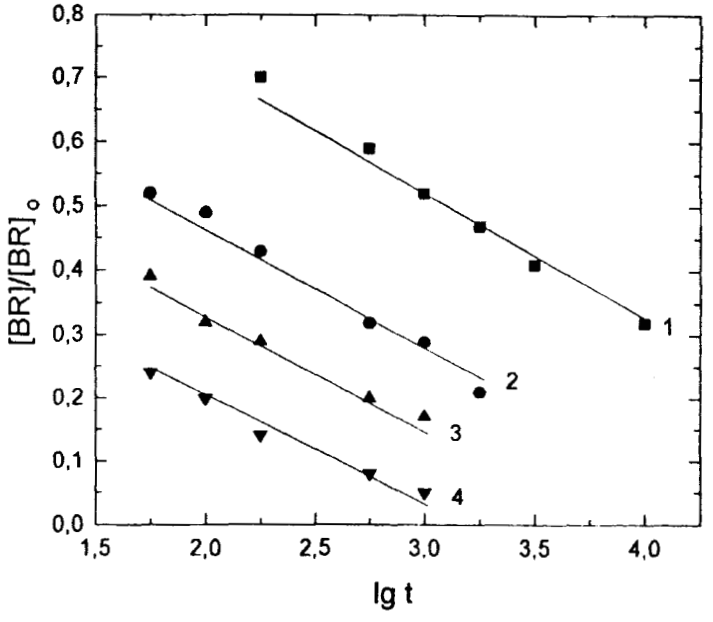

FIGURE 17 Kinetics of BR decay in PMMA at 1–183 K, 2–193 K, 3–203 K and 4–218 K.

The distribution of frequency factors are overlapped too. Thus the conversion limiting steps of BRs and carbenes with the lowest reactivity are controlled in micropores by the same molecular dynamics, namely the torsional movements of the main chains.

The results obtained reveal the determining role of the carbene rotational motions concentrated in micropores of polymers in BR formation. In this regard such reaction may be considered as a special probe to study the molecular dynamics at low temperatures. It is known that the traditional spin probe method is intended to obtain the information about molecular motions at a temperature near and above the glass temperature. At temperatures lower than T_g of the rotational frequencies the ESR method resolves only the high frequency part of the paramagnetic probes. The development of ESR with the transfer of saturation allows us to extend the interval of reliable determinations of the spin probe correlation times to the region of slow motions ($\tau = 10^4$ s) at $T < T_g$.

c. The Molecular Products of the Carbene Reactions in Polymers

The analysis of the molecular product composition is one of the principal methods to study the mechanism of the carbene reactions in solid polymers. But a set of methods applied for this purpose is limited by low solubility of the carbene precursors. UV and IR methods are most important for the identification of groups grafted on macromolecules in the carbene reactions on condition that molecular extinctions are reasonably high. Apart from spectral techniques the mechanism of the carbene reaction product formation in polymers can be established by the measurement of the insoluble gel fraction formed during the cross-linkage of macromolecules by biscarbenes. In this case the conversions of diazocompounds into products are directly exhibited by the gel fraction yield.

The irradiation of PMMA films with QDA by light with $\lambda \approx 365$ nm at 295 K results in the appearance of new UV absorption band at 275 nm [22] (Fig. 18) which is typical of phenols. The bnads of the hydroxyl groups (3440 cm^{-1}), C—H bonds (1596 cm^{-1}) and C=C (1500 cm^{-1}) of the phenol aromatic ring arise in the IR spectrum. The phenol formation is also observed in PMMA films as a result of the

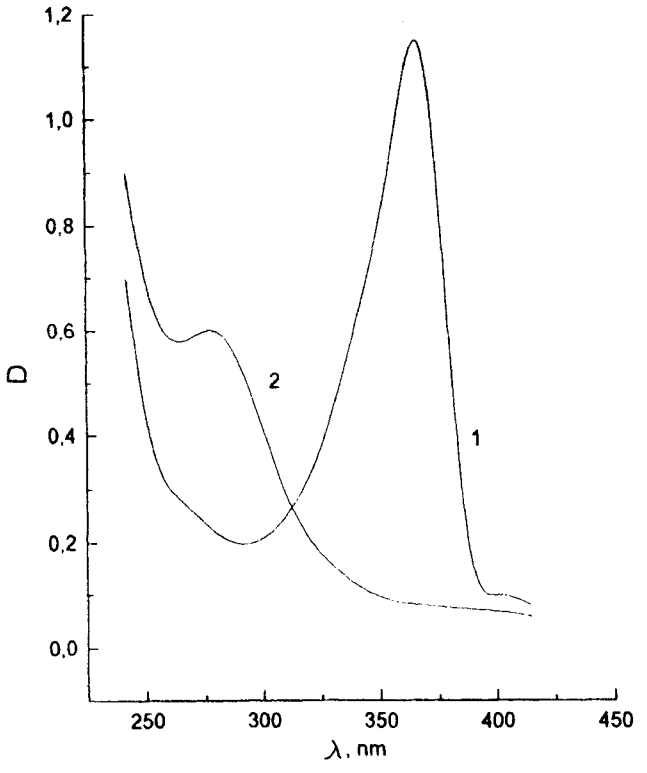

FIGURE 18 UV spectra of PMMA with QDA (1) and after irradiation by light $\lambda \sim 363$ nm at 295 K (2).

CHC decay at $T > 77$ K. The detectable decrease of the phenol absorption band was not detected in the course of the reprecipitation of samples irradiated at 295 K and 77 K by ethanol, suggesting that these phenol groups are chemically bonded with macromolecules.

As discussed above the low temperature reactions of ^{3}CHC involve the RP and isolated radical formations by the hydrogen atom abstraction from C—H bonds of the PMMA ester groups. The subsequent recombination of RP must give rise to the respective product $\sim CH_2C(CH_3)(COOCH_2C_6H_4OH)CH_2\sim$. At 295 K CHC, resulting in the singlet state in primary reaction of the QDA photodecomposition, can either immediately react with macromolecules with the formation of the insertion product, or transform to the ground triplet state in time of 10^{-10} s[5]. The comparison of the UV intensities of

initial and irradiated samples shows that the CHC conversion occurs quantitatively in the insertion product at 295 K and 77 K in the range of $[QDA] = 10^{-3} - 10^{-1}$ M and is not followed by formation of other compounds such as diphenoquinone or *p*-benzoquinone as result of two CHC recombinations or CHC oxidation.

A similar product was observed in OP with QDA during irradiation by light with $\lambda \approx 365$ nm. The absorption band with $\lambda_{max} \approx 280$ nm results in UV spectrum. The same band was detected in OP irradiated by light at 77 K after the warming to the room temperature. The phenol groups are chemically bonded with macromolecules since repeated extracting by ethanol did not lead to the disappearance of 280 nm band. The reaction product has the following structure $\sim CH_2CH{=}CHC(C_6H_4OH)(CH_3)\sim$. We emphasise that in this sytem the products of CHC attaching to double bonds are not noted [59]. The formation of these products, however, must not be excluded. But, as was shown in work [60], such spirocyclohexadienones are extraordinary sensitive to impurities of acids and bases and can be easy isomerised at room temperature with the cycle decomposition into phenols.

Consider now the results of the investigation of the thermal and photochemical transformation of BQDA in PVA. The currently available evidence [59] suggests that cyclohexadienone carbenes are able react with alcohols giving hydroquinone esters $(OH)C_6H_4(OR)$. The band of BQDA with $\lambda_{max} \approx 360$ nm disappears during the film irradiation by light with $\lambda > 300$ nm and the heating from 320 K to 363 K. As this takes place, the films partly lose the water solubility and the band with $\lambda_{max} = 290$ nm belonging to the hydroquinone ester [61] makes their appearance in the UV spectrum of insoluble fraction. On the strength of these results the assumption was made that the cross-linkage takes place owing to the BCHC insertion into PVA hydroxy groups. For simplicity the cross-linkage process can be presented in the following manner

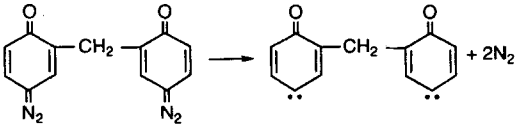

(32)

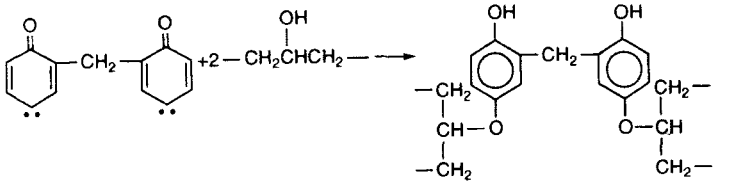

(33)

An alternative mechanics of the cross-linkage connected with the recombination of PVA macroradicals and phenoxy radicals is also possible

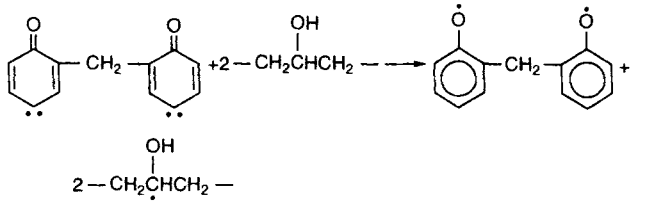

(34)

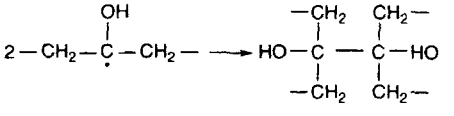

(35)

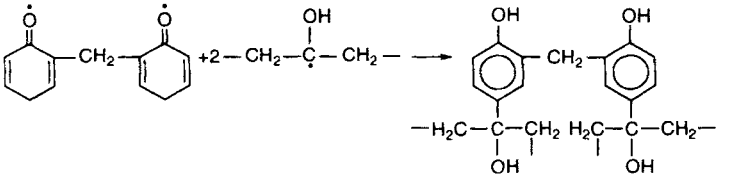

(36)

In all probability the cross-linkage reactions (35) and (36) do not play an important role because of the water insoluble films are easy dissolved at the heating in the concentrated hydrogen chloride acid. It is common knowledge [62] that this acid is capable of the phenol ester cleavage on evidence derived from ESR. Besides, the interaction of macroradicals and phenoxy radicals by reactions (35), (36) does not result in cross linking. Macroradicals $\sim CH_2C(OH)CH_2\sim$ and phenoxy radicals were registered at 77 K by ESR. The formation of these radicals is explained by the transition of primary singlet

carbenes to the ground triplet state when they are able to abstract the hydrogen atom from C—H bonds. It should be noted that no RPs with the average distance between radicals of 0.5–0.6 nm in PVA were detected. Likewise no mono and biscyclohexadienone carbenes were registered. These facts testify that the high reactivity BCHC in the hydrogen abstraction and high efficiency of the radical egress from cages exist even at 77 K. The isolated radicals can decay on PVA warming-up without the cross-linkage. Consequently, one can believe that the macromolecule cross-linkage is a result of the reaction of the singlet BCHC insertion into O—H bonds. The rate of the gel fraction formation is significantly diminished with the temperature decrease. The cross-linkage is observed in samples after the total photolysis of BQDA (10 min). It is evident from plots shown in Figure 19a that during BQDA photodecomposition the cross-linkage is linearly related to the degree of the adding conversion. The carbenes are likely to be involved in an alternative specific reaction. They react in the triplet state by reaction (34) with the formation of radicals that are transformed into some products.

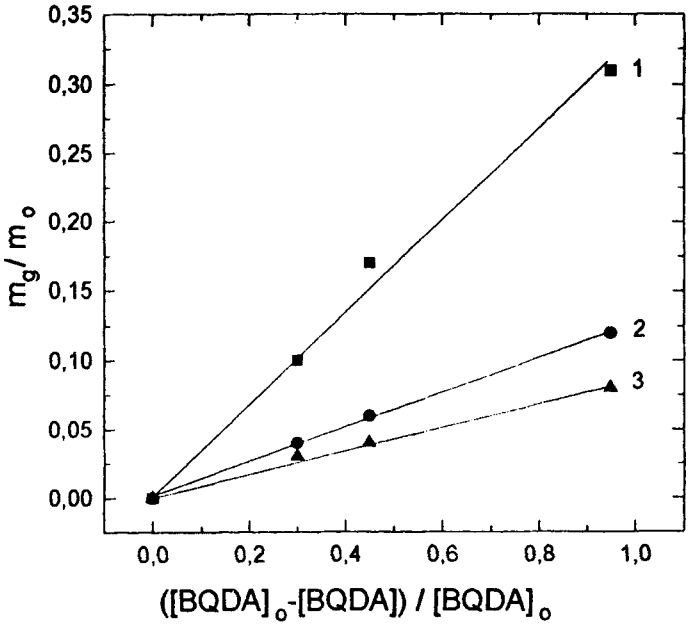

a)

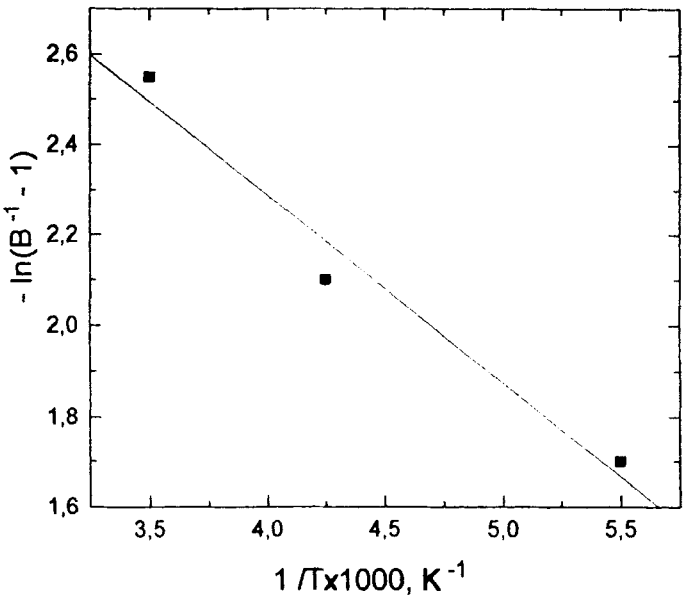

b)

FIGURE 19 The dependence of gel formation in PVA on BQDA photodecomposition degree at 1–295 K, 2–243 K, 3–183 K (a) and temperature dependence of parameter B (b).

The main carbene reactions in PVA initiated by BQDA photolysis can be represented by following scheme

$$\text{BQDA} \longrightarrow {}^1\text{BCHC} + \text{RH} \xrightarrow{k_1} \text{S} \tag{37}$$

$$k_{ST} \uparrow\downarrow k_{TS}$$

$${}^3\text{BCHC} + \text{RH} \xrightarrow{k_2} \dot{\text{R}} \longrightarrow \text{products} \tag{38}$$

It was found that the optical density of band with $\lambda_{max} = 290$ nm associated with by the cross-linkage groups is similarly changed as the insoluble fraction m_g. Therefore, $m_g/m_0 = \delta[S]$, where S is cross-linkage, m_0 is the film weight. In the case that the carbene concentration is at steady-state at relatively by high temperatures of 183–295 K the gel fraction yield should be expressible as

$$\frac{m_g}{m_0} = \frac{[\text{BQDA}]_0 k_1 k_{TS}}{k_1 k_{TS} + k_2 k_{ST}} \left(1 - \frac{[\text{BQDA}]}{[\text{BQDA}]_0}\right) \tag{39}$$

From the plots in Figure 19a it follows that the efficiency of crosslinking, defined by $B = k_1 k_{TS}/(k_1 k_{TS} + k_2 k_{TS})$, is changed from 0.9 at 295 K to 0.08 at 183 K. The temperature dependence of B can be represented as

$$\ln\left(\frac{1}{B} - 1\right) = A + \frac{\Delta E_{TS} + E_1 - E_2}{RT} \tag{40}$$

where A is constant (Fig. 19b).

The retention of this relationship over a fairly wide range of temperatures proves the suggested mechanism of BQDA conversion. The difference of effective activation energies, including ΔE_{TS}, is 2.8 kJ/mol. By this is meant that $E_2 - E_1 < \Delta E_{TS}$. Therefore, the decrease of the efficiency of the cross-linkage by the lowering of the photolysis temperature results from the increase of the relative population of the ground triplet state similarly to the temperature dependence of the product composition in the solid phase reaction of DPC with isobutylene [8]. A build-up of the gel fraction after the BQDA photodecomposition may be attributed to initiation of cross-linkage of products resulting in the carbene reaction (38).

The considerable distinctions of the cross-linkage were observed at the BQDA thermal decomposition. The kinetics of this process is controlled by the first order law at 320–373 K with the rate constant $k = 5\ 10^{10} \exp(-85.6\ \text{kJ/RT})$, s^{-1} (Fig. 20). In this case insoluble fraction is formed in the wake of the BQDA complete decay similarly to photolysis. As this takes place, the contribution of the BQDA conversion products in cross-linkage is the more important the higher the temperature. The amount of gel fraction in PVA is proportional to BQDA decomposed to the high conversion extent (Fig. 21). Hence, the efficiency of cross-linkage is equal at different temperatures and accounts for 0.3. As the yield of products is increased late in the BQDA decay, the abrupt rise of the cross-linkage takes place. Assuming that the singlet-triplet equilibrium for carbenes is applicable to the BQDA photolysis one can allow their involvement in two competitive reactions. One produces at once the cross-linkage as a result of the

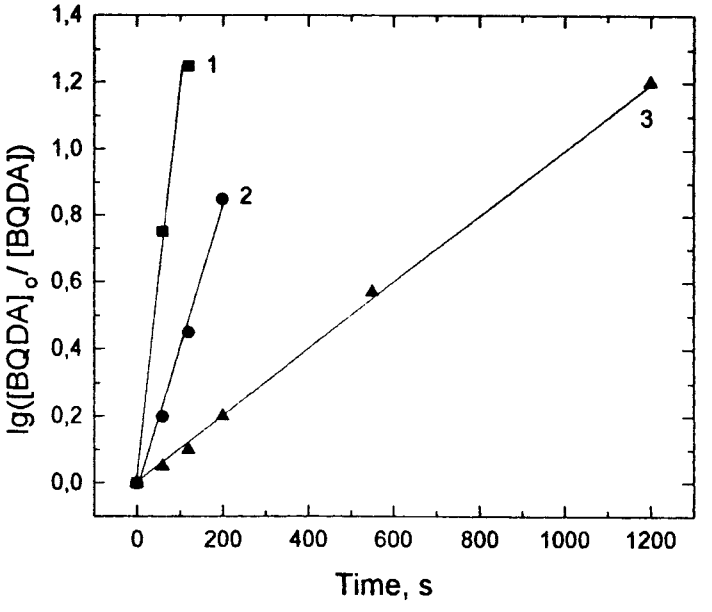

FIGURE 20 Kinetics of BQDA thermal decomposition in PVA at 1–373 K, 2–343 K and 3–322 K.

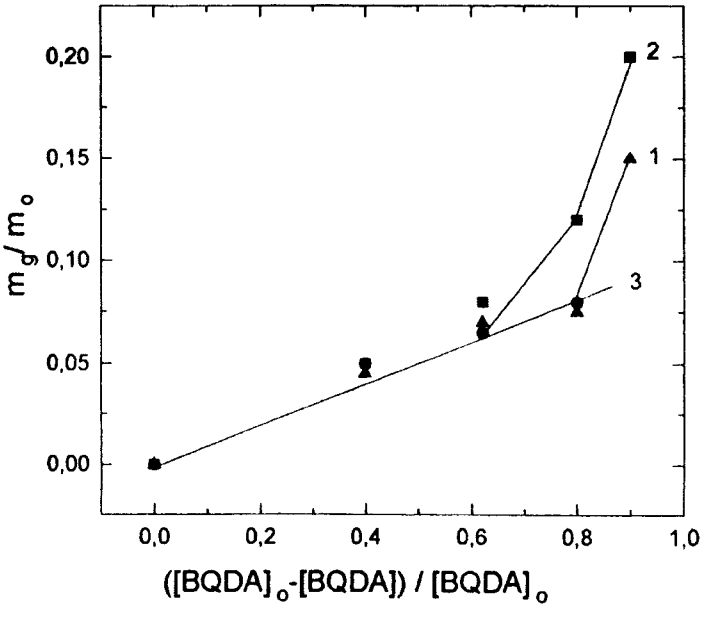

FIGURE 21 The dependence of gel formation in PVA on BQDA thermal decomposition degree at 1–373 K, 2–343 K and 3–322 K.

singlet BCHC insertion in O—H groups of macromolecules and other reaction of triplet BCHC gives some other product. Since the gel formation efficiency during the BQDA thermal decomposition does not depend on temperature and is threefold smaller than during photolysis at 295 K, the mechanism of reaction (38) is not applicable. The absence of the temperature dependence for the gel yield implies that $\Delta E_{TS} + E_1 = E_2$ in equation (40), and the triplet carbenes react effectively at high temperatures with larger activation energy than at low temperature conversions. Besides, the reaction product must itself undergo cross-linking during heating as evidenced by a drastic gain of the gel formation at high degree of the diazocompound decay (Fig. 21).

It is possible that the intramolecular hydrogen atom transfer occurs from methylene group of triplet BQDA.

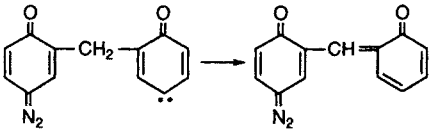

(41)

Such reactions of intramolecular rearrangement with the participation of the hydrogen atom are characteristic of carbenes [63]. By reaction (41) the monodiazocompound containing the methylene quinone group is formed. On further transformation it gives the corresponding product of insertion in O—H bond of PVA.

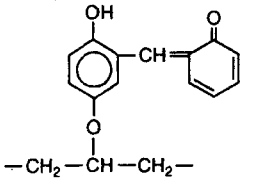

In turn the methylenequinone groups of these products are capable to react with hydroxy groups of macromolecules.

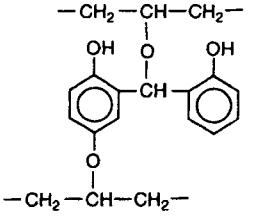

In support of this conclusion one can note that a typical reaction of low molecular alcohols with methylequinone is the formation of ether $(OH)C_6H_4(CH_2OR)$ [64]. The data obtained show the mechanism of influence of the polymer matrix physical condition on the carbene reactivity. PVA shows at the glass transition temperature much high intensity of molecular movements than at room and or cryogenic temperatures. The different kinds of relaxation processes correspond to these temperature ranges. So the interval of 320–370 K is characteristic of glass transition in randomly packed sites of PVA and the range of 180–279K corresponds to the relaxation of the hydrogen-non-bonded macrochains [65]. The distinctions, observed for the PVA cross-linkage by the BQDA photo and thermal decompositions are analogous to the effect of the low molecular alcohol phase state on products of the carbene reaction [10]. In going from the rigid matrix to $T > T_g$ the change of the triplet carbene conversion mechanism takes place. The bimolecular reaction of the hydrogen atom abstraction is suppressed and the peculiar intramolecular reaction of BQDA takes place. This, suggests that the PVA matrix effect on the carbene reactions is defined by the dependence of their mechanism on molecular relaxation. The change of the product composition of the carbene reactions in polymers may be observed within one phase state in the context of numerous relaxation processes.

d. The Kinetics of the Carbene Reactions in Filled Polymers

The filling is one of the most commonly encountered way of the polymer modification. The experience thus far gained shows that the filler effect enhances the polymer volume non-uniformly [66] through formation of interfaces physical structures of which is different from those in the volume.

The information on the polymer interfaces can be obtained from the characteristics exhibiting the essential dependence on the filling degree. In the context of the close association between the polymer structural-physical properties and the kinetics of the radical reactions the determination of kinetic plots may be considered as an appropriate technique of the structural characteristic assessment in particular of the interface effective thickness. The studies on thermal and thermoxidational degradation of the filled polymers [67] show a

pronounced role of filler in these processes. But in the high temperature reactions of oxidation the catalytic properties of filler surface can influence also the reaction kinetics besides the structural-physical factors. From this viewpoint the implementation of the low-temperature cage radical reactions, specifically the carbene reactions, has the advantage, because these reactions reflect primarily the molecular organisation features of interfaces. Evidently they are not complicated by the interaction of radicals with the filler surface.

In Figures 22a, b the kinetic curves of DTBCHE decay at 100 K in PMMA and AC containing up to 65 mass percentage of aerosil are shown. Here, the introducing of filler reduces the rate of DTBCHC decay in both polymers. The similar effect was observed throughout

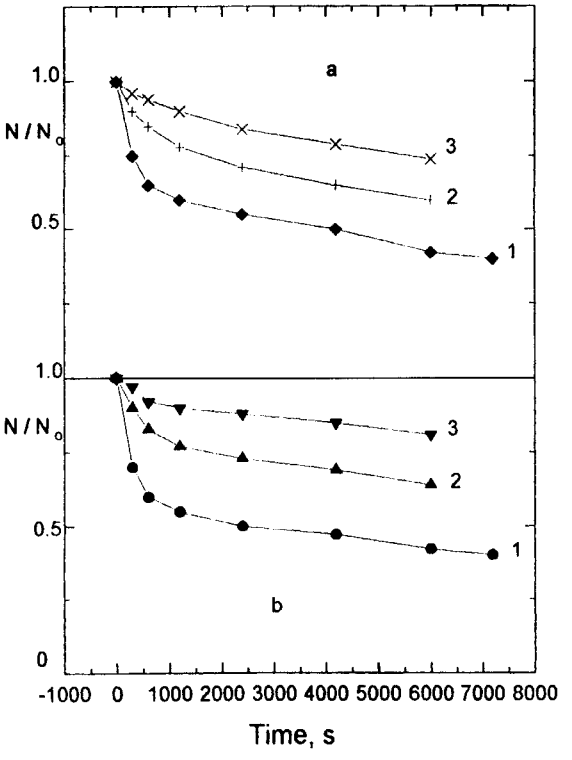

FIGURE 22 Kinetics of DTBCHC decay at 100 K in PMMA (a) and AC (b) with 1–1, 2–40 and 3–65% of aerosil.

the entire temperature range of 100–140 K. In the studied temperature range these curves are satisfactorily straightened in co-ordinates of (10) (Figs. 23a, b).

With the filler content increase the limiting values of the rate constants k_{max} and k_{min} in PMMA and AC are decreased but the parameter of the distribution width is kept constant. At 1000 K $\lg(k_{max}/k_{min})$ are 6.8 and 5.5 respectively in PMMA and AC. The distribution becomes much narrower with increased temperature. The constant distribution width of the DTBCHC decay rate in samples with the different filling is important to understand the nature of the structural-physical modification of polymers. This conclusion has been confirmed by the other method of kinetic analysis involving the approximation by equation put forward in work [68].

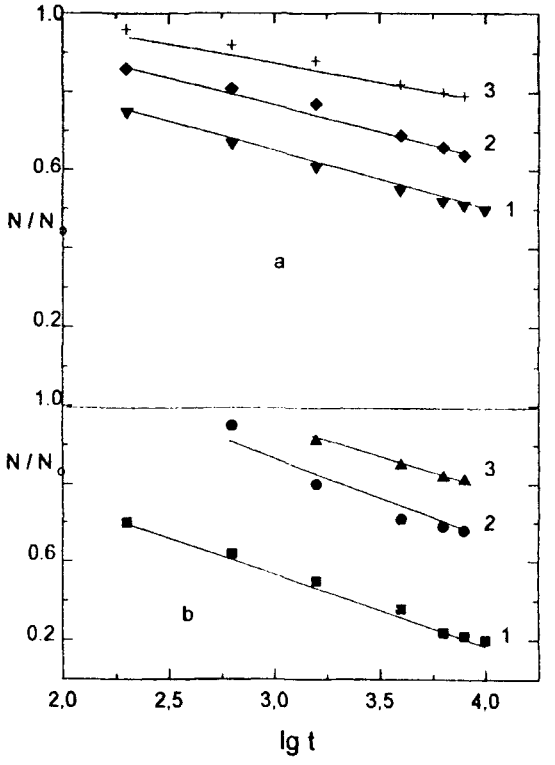

FIGURE 23 The linear approximations of kinetics of DTBCHC decay in filled PMMA (a) and AC (b) with 1–1, 2–40 and 3–65% of aerosil.

Note that

$$\frac{N}{N_0} = (1 + nk_0t)^{-1/n} \tag{42}$$

where k_0 is the DTBCHC average effective rate constant obtained on the basis of distribution by the decay rate constants $\rho(k_{ef})$: $k_0 = \int k_{ef}\,\rho(k_{ef})dk_{ef}$, n is parameter determining the distribution width. In Figure 24 the straightenings of the carbene decay kinetics are shown at 100 K in co-ordinates of (42). All curves are approximated by the same anamorphosis regardless of the aerosil content and, therefore, n is constant. The kinetic parameter values obtained are listed in Table III. Thus the kinetic analysis performed by two

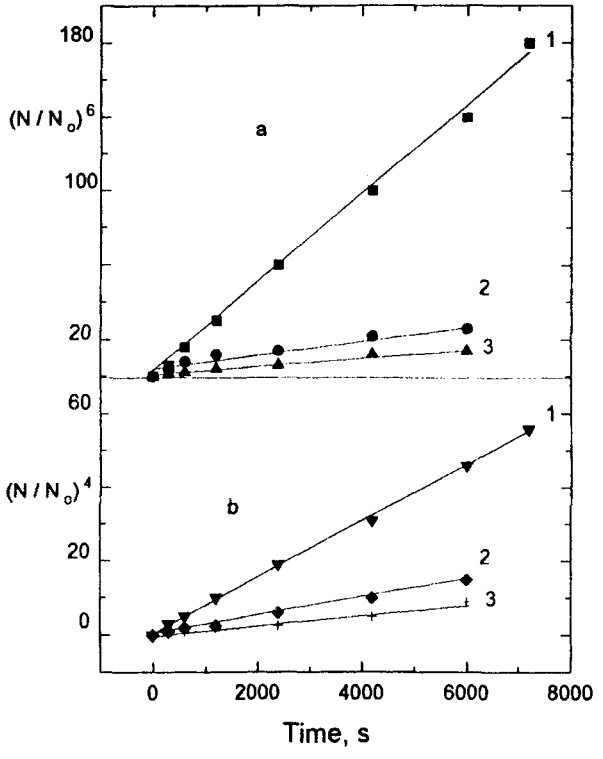

FIGURE 24 The linear approximations of DTBCHC decay kinetics in filled PMMA (a) and AC (b) in co-ordinates of (42) with 1–1, 2–40 and 3–65% of aerosil.

TABLE III Kinetic parameters of DTBCHC decay in filled PMMA and AC

T, K	*aerosil*, %	$k_0\,10^4$, s^{-1}	*n*
	PMMA		
100	1	28.0	6
	25	14.5	
	40	4.2	
	65	1.6	
113	1	35.0	4
	25	25.0	
	40	14.7	
	65	1.8	
125	1	38.0	2
	25	25.0	
	40	16.7	
	65	2.1	
	AC		
100	1	13.0	4
	25	11.8	
	40	2.5	
	65	0.7	
125	1	140.0	3
	25	–	
	40	87.0	
	65	6.9	
135	1	1000	2
	25	580	
	40	200	
	65	12	

methods gives the same result: the distribution by the effective rate constants of the DTBCHC decay in filled polymers does not depend on the filler content.

Figures 25a, b show relationships of the average rate constant k_0 and distances between the filler particles. These distances were estimated by equaion [66]

$$l = d\left[\left(\frac{0.8}{l-\xi}\right)^{1/3} - l\right] \tag{43}$$

where d is the diameter of the aerosil particles (≈ 20 nm), ξ is the aerosil volume fraction in polymer. As is seen from figure, the k_0

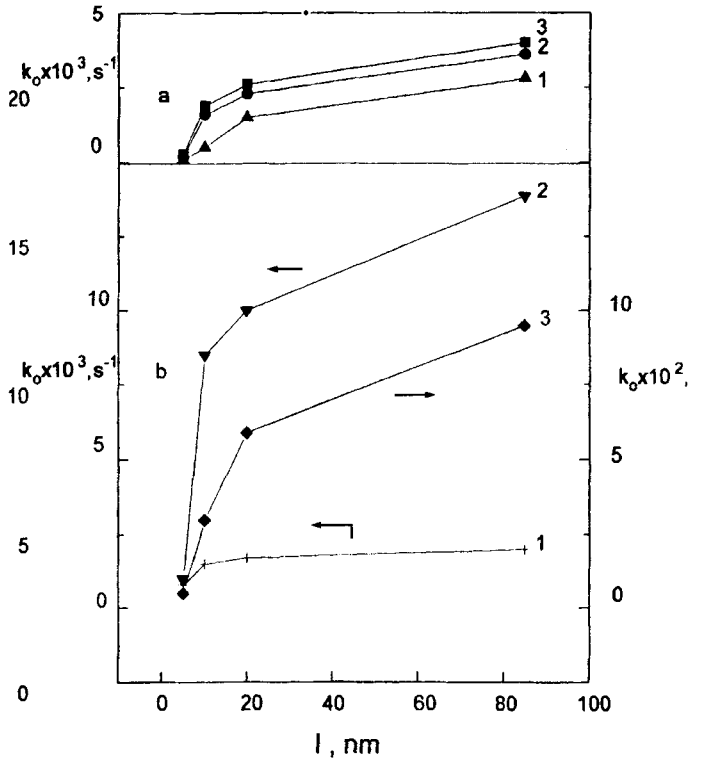

FIGURE 25 Relationships of average rate constant on distances between aerosil particles in PMMA at 1–100 K, 2–113 K, 3–125 K (a) and AC at 1–100 K, 2–125 K, 3–135 K (b).

values are moderately decreased with the filler content increase in the range of l exceeding 20 nm. If $l < 20$ nm, k_0 is decreased more than tenfold.

Along with the physical structure modification of polymers the filler effect on kinetics of the DTBCHC decay can be also caused by the change of mechanism on surface. For instance, one can allow that the fraction of carbenes on surface decay with a smaller rate as compared with reaction in the polymer volume. A special experiment was made to elucidate the association of the filler effect with this reason. The sample of the filled polyvinylpyrrolidone was prepared with the DTBCHC precursor tentatively coated on aerosil surface. In this sample irradiated at 77 K by light with 300 nm $< \lambda <$ 400 nm, the kinetics of the DTBCHC decay was studied at 100–125 K. It turns

out that the value of the average rate constant for these samples is two-threefold higher. Therefore, the decay rate increase of carbenes on surface is not due to recombination because of the average distance between them is 3 nm and the DTBCHC decay on surface must cause the opposite filler effect. Thus we can conclude that the carbene decay in filled polymers takes place mainly in reaction with macromolecules. The essential decrease of this process rate with the increasing of the aerosil content must be associated with the physical structure changes in polymers accounting for by transformations in the interface state. Its thickness estimated by plots of Figure 25 is 15–20 nm.

On the basis of kinetic data obtained the following conclusions can be reached about the nature of the matrix structure changes by filling. As the width distribution by the DTBCHC reactivity is not changed with the conversion of polymer into the interface state the structural-physical modification does not influence the distribution of the rate constants of primary reaction of the hydrogen atom transfer from C—H bonds of macromolecules to carbenes (18) which is the limiting step of their decay. This step, however, determines the kinetic non-equivalence of carbenes in reaction with macromolecules through the dispersion of distances between the carbene centre and C—H bonds of matrix. In this connection one can conclude that the structural changes by filling effect the efficiency of the intermediate RP recombination defined by $[(k_1 P_T/k_2 P_S) + 1]$ in (19). It was found that as the filled polymer is prepared from solution the formation of more brittle packing of macromolecules is possible in interfaces [66]. Such structural realignment can change the relation between the recombination rate of singlet RP and back hydrogen atom transfer together with the relative population P_T/P_S as a result of the RP configuration changes [39].

THE THERMOSTABILISATION OF POLYISOPRENE BY THE PHENOL GRAFTING IN THE CARBENE SYNTHESIS

A convenient method of stabilizer fixation in polymers is the reaction of suitable carbenes with macromolecules. This method avoids physical losses of stabilizers due to volatilisation and washing-off by water and other organic solvents. The grafted antioxidants can be effective

under service conditions of polymeric materials at high temperatures and also during reprocessing. There are examples of effective use of carbenes to stabilize polyolefines by 2,6-di-t-butylphenol (DTBP). The fixed phenol shows better protective properties at 300–500 K than non-grated phenols [70].

To fix DTBP on polyisoprene (PI) films with DTBQDA additives ($6.10^{-3} - 4.10^{-2}$ M) were heated for one hour at 343 K [71]. In this case the appearance of the 280 nm phenol band in UV spectrum is observed. The reprecipitation of PI samples does not lead to the band disappearance. The estimation shows that the phenol concentration is about 90% of that of DTBQDA inserted in PI. The oxidation of PI with grafted DTBP at 353 K and 363 K was performed on 50μ films placed on CaF_2 plates. The thermoxidation kinetics was determined by the accumulation of the carbonyl (1720 cm^{-1}) and hydroxyl (3200–3600 cm^{-1}) absorptions in IR spectrum and by the oxygen sorption. The oxidation of PI stabilised by 2,6-di-t-butyl-4-methyl-propionatphenol (DTBMP) was studied by the same technique to compare both antioxidants from the view of their stabilizing capabilities.

The formation of phenol derivatives in carbene synthesis is possible in PI by reactions of triplet carbenes with C—H allyl bands and as a result of spirodienone conversion [72]

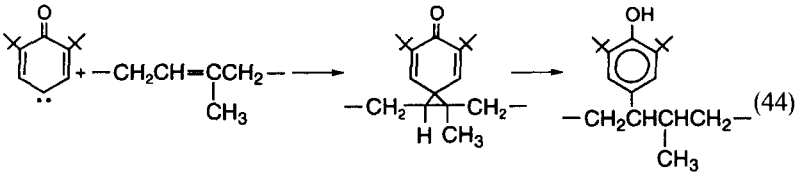

(44)

The kinetic curves of carbonyl group accumulation in PI with DTBP are shown in Figure 26. The same type of curves were obtained for hydroxyl products and oxygen sorption.

The dependence of induction periods of oxidation on grafted antioxidant concentrations is shown in Figure 27. The analogous relationships are presented for low-molecular phenol. The observed concentration dependence shows large and significant differences. The induction period is increased linearly for grafted antioxidant with concentration. The evident departure from linearity was observed for DTBMP in the concentration range up to 3.8 10^{-2} M. The induction

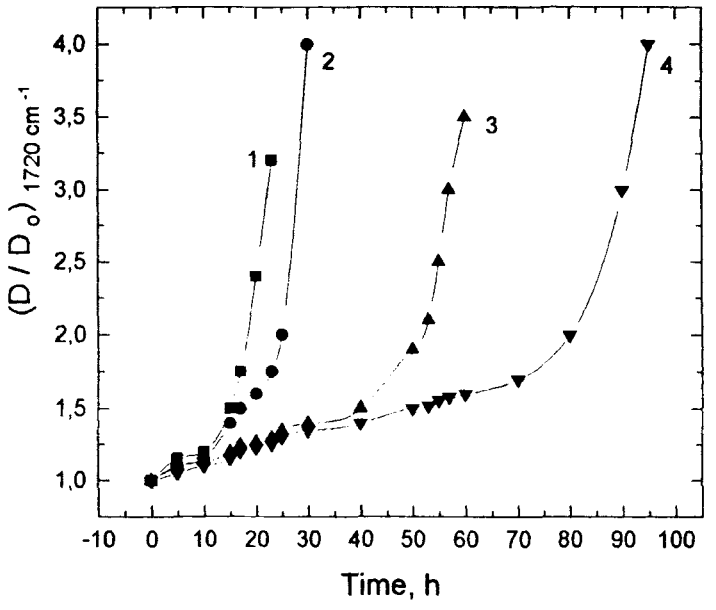

FIGURE 26 Kinetics of C=O formation of 353 K in PI with grafted DTBP: 1–6.36 10^{-3} M, 2–1.27 10^{-2} M, 3–2.12 10^{-2} M, 4–4.24 10^{-2} M.

priod values are close for both antioxidants at low concentrations. The difference of τ rises largely with the antioxidant concentration increase. This result suggests that the deviation from linearity of the concentration dependence of τ for DTBMP does not result from the sweating-out that is typical for low-molecular antioxidants.

It is known that the dependence of τ on the inhibitor concentration of thermoxidation is defined by the kinetics of antioxidant consumption. Thus, PhOH consumption with constant rate corresponds to the linear concentration dependence of τ [73, 74]. The kinetics of phenol consumption does not fall from the zero order until the end of the induction period when the phenol concentration is approached to a critical value. Yet neither the proportionality of the induction period values and phenol concentrations nor the zero order of its consumption kinetics are commonly encountered in practice.

The origin of this effect consists in unexpected side reactions with assistance of phenoxy radicals, resulting at the termination of oxidation chains [75], as well as direct interaction of phenols with oxygen in the course of inhibited oxidation [76]. One can consider possible

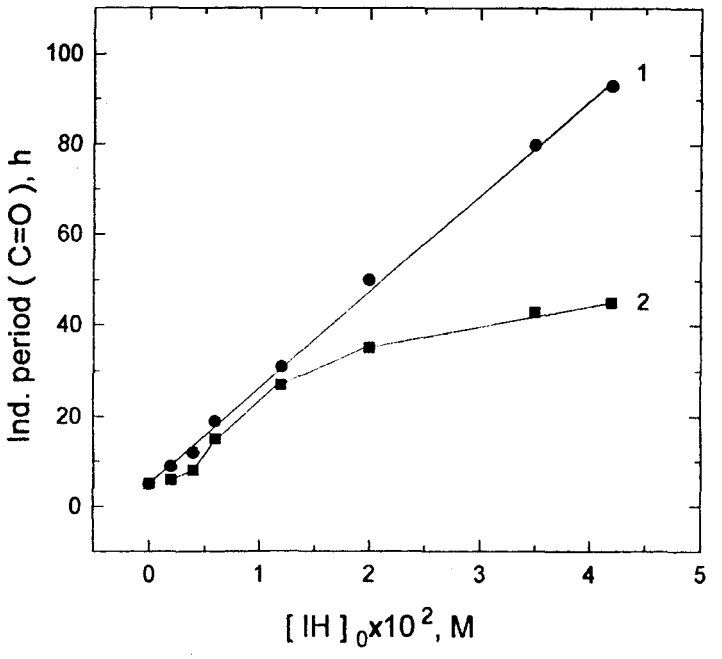

FIGURE 27 The dependence of τ of C=O formation at 353 K in PI on antioxidant concentrations: 1-grafted DTBP, 2-DTBMP.

reasons resulting in the decrease of DTBMP antioxidational activity in PI as compared with grafted DTBP. The direct oxidation of low-molecular weight phenol is ruled out because this process does not table place with its grafted analogue. The possibility of β-dissociation of phenoxy radicals with substitutes in the *p*-position can be assumed with the result that slightly active inhibitor radicals are converted to active substitute radicals. Similar reactions are typical of *p*-alkoxy derivatives of phenols [77]. Then the PhOH consumption is accelerated greatly in the range of the phenol high concentrations. This reaction can be ignored for phenoxy radicals containing alkyl substitutes in *p*-position [77]. Thus, grafted DTBP is not affected by undesirable β-dissociation decreasing its efficiency.

The comparison of activity of traditional and grafted antioxidants shows that the latter has qualitative advantages in addition to non-volatility. The grafted DTBP is an "ideal" antioxidant in the overall studied concentration range, the upper limit of which corresponds to

concentrations used in real working conditions. Its consuption within the induction period occurs as a result of linear termination of oxidation chains and is evidently not accompanied by side reactions. These advantages favor the use of hindered phenols grafted by carbene synthesis on macromolecules to stabilise PI and other elastomers.

CONCLUSION

One can note a series of the common features of the carbene reactions in solid polymers. The physical sturcture of medium results in the non-equivalence of carbene reactivity and non-uniformity of distribution of the carbene precursors. The main reason of kinetic non-equivalence is the space-orientation variety of the carbene centre arrangement with relation to the C—H bonds of the matrix. This variety defines the dispersion of the rate constants of the hydrogen atom transfer at low temperature. This reaction is described by the model of the hydrogen atom tunneling through the potential barrier oscillating in response to intermolecular vibrations.

A fraction (up to 20%) of carbenes is clustered in two, three or more particles both in polymers and frozen organic glasses. The dimerisation, trimerization and so on with the BR formation takes place in such clusters. But the mechanism of the carbene transformation in polymers has essential dissimilarity determined by molecular organisation. The stepwise kinetics of the low temperature carbene decay in polymers is often governed by the law "degree of conversion-logarithm of time". The dispersion of $3-5\ 10^{-2}$ nm in equilibrium distances between carbene and the C—H bonds of macromolecule accords to the difference in 5–6 orders for the carbene decay rate constants.

The established strong structure effect on the carbene reactivity allows us to use their reactions as a sensitive technique to study the structural-physical characteristic of polymers. One can determine in part the interface thickness of filled polymers by the kinetic data of the triplet carbene decay. The reaction of the BR formation in clusters of arylcarbenes allows us to study molecular dynamics at cryogenic temperatures. The kinetics of this process reflects a very wide spectrum of the orientational movement frequencies from 10^5 to 10^{-6} s^{-1}.

In parallel with investigation of the cage environment influence on kinetics of elementary reactions in solid polymers carbenes can be used for solving practical problems of stabilisation of rubbers by grafting of hindered phenols.

References

[1] Siddiqui, S. and Cais, R. E. (1986). *Macromolecules*, **19** (3), p. 595–603.
[2] Bradbury, J. H. and Perera, M. C. S. (1986). *British. Polym. J.*, **18** (2), p. 127–134.
[3] Aglietto, M., Alterio, R., Bertani, R., Galleschi, F. and Ruggeri, G. (1989). *Polymer*, **30**, 6, p. 1133–1136.
[4] Emanuel, N. M. and Buchachenko, A. L. (1988). Chemical physics of molecular degradation and stabilization of polymers, Moscow, Nauka, p. 133.
[5] Kovarsky, A. L. and Saprygin, V. N. (1984). *Vysokomolek. Soed.*, **A 29** (9), p. 1949–1956.
[6] Skell, P. S. (1985). *Tetrahedron*, **42** (8), p. 1427–1428.
[7] Hoffman, O. R. (1969). *J. Amer. Chem. Soc.*, **90** (6), p. 1475–1485.
[8] Wright, B. B. (1985). *Tetrahedron*, **42** (8), p. 1517–1523.
[9] Moss, R. A. and Dolling, U. H. (1971). *J. Amer. Chem. Soc.*, **93** (4), 954–960.
[10] Tomioka, H., Inagaki, T., Nakamura, S. and Izawa, Y. (1979). *J. Chem. Soc. Perkin I*, **1**, p. 130–134.
[11] Tomioka, H., Griffin, G. W. and Nishigama, K. (1979). *J. Amer. Chem. Soc.*, **101** (20), p. 6009–6012.
[12] Palik, E. C. and Platz, M. S. (1983). *J. Org. Chem.*, **48** (7), p. 963–969.
[13] Boxer, S. G., Chidsey, C. E. D. and Roelofs, M. G. (1982). *J. Amer. Chem. Soc.*, **104** (9), p. 2674–2675.
[14] Schevelev, V. A. (1971). *Vysokomolek. soed.*, **A 13** (10), p. 2316–2323.
[15] Platz, M. S., Senthilnathan, V. P., Wright, B. B. and McCurdy, C. W. (1982). *J. Amer. Chem. Soc.*, **104** (24), p. 6494–6501.
[16] Platz, M. S. (1989). *Acc. Chem. Res.*, **21** (6), p. 236–242.
[17] Iwasaki, M. and Toriyama, K. (1967). *J. Chem. Phys.*, **46** (7), p. 2852–2853.
[18] Iwasaki, M., Ichikawa, T. and Ohmori, T. (1969). *J. Chem. Phys.*, **50** (5), p. 1984–1990.
[19] Pudov, V. S., Yasina, L. L. and Buchahenko, A. L. (1974), *Kinetika i kataliz*, **15** (5), p. 1110–1114.
[20] Wright, B. B. and Platz, M. S. (1984). *J. Amer. Chem. Soc.*, **106** (15), p. 4175–4180.
[21] Wright, B. B., Kanakarajan, K. and Platz, M. S. (1985). *J. Phys. Chem.*, **89** (16), p. 3574–3577.
[22] Vorotnikov, A. P., Davydov, E. Ya. and Toptygin, D. Ya. (1984). *Vysokomolek. Soed.*, **B 26** (9), p. 664–669.
[23] Siebrand, W. and Wildman, A. T. (1986). *Acc. Chem. Res.*, **17** (1), p. 238–243.
[24] Vorotnikov, A. P., Davydov, E. Ya., Pariyskii, G. B. and Toptygin, D. Ya. (1983). *Khimicheskaya Fizika*, **2** (6), p. 818–822.
[25] Korshak, V. V., Vorotnikov, A. P., Davydov, E. Ya. Kozyreva, N. M., Kirillin, A. I., Skubina, S. B. and Toptygin, D. Ya. (1986). *Dokl. Akad. Nauk SSSR*, **291** (2), p. 376–381.
[26] Lebedev, Ya. S. (1978). *Kinetika I kataliz*, **19** (6), p. 1367–1376.
[27] Vorotnikov, A. P., Davydov, E. Ya. and Toptygin, D. Ya. (1985). *Izv. Akad. Nauk SSSR, ser. khimich.*, **6**, p. 1275–1281.
[28] Vorotnikov, A. P., Davydov, E. Ya. and Toptygin, D. Ya. (1983). *Izv. Akad. Nauk SSSR, ser. khimich.*, **7**, p. 1499–1505.
[29] Le Roy, R. J. (1980). *J. Phys. Chem.*, **84** (26), p. 3508–3521.

[30] Trakhtenberg, L. I., Klochikhin, V. L. and Pshezhetsky, S. Ya. (1981). *Chem. Phys.*, **59** (1), p. 191–198.
[31] Lippincott, E. R. and Schroeder, R. (1955). *J. Chem. Phys.*, **23** (8), p. 1131–1141.
[32] Brunton, G., Griller, D., Barclay, K. R. and Ingold, K. U. (1976). *J. Amer. Chem. Soc.*, **98** (22), p. 6803–6807.
[33] Klochikhin, V. L. and Trakhtenberg, L. I. (1983). *Khimicheskaya Fizika*, **2** (6), p. 810–817.
[34] Vorotnikov, A. P., Davydov, E. Ya. and Toptygin, D. Ya. (1987). *Khimicheskaya Fizika*, **6** (5), p. 639–644.
[35] Davydov, E. Ya., Vorotnikov, A. P. and Toptygin, D. Ya. (1990). *Int. J. Polym. Mat.*, **13** (1), p. 191–194.
[36] Steiner, U. E. and Ulrich, T. (1989). *Chem. Rev.*, **89** (1), p. 51–147.
[37] De Kanter, F. J. J. and Kaptein, R. (1982). *J. Amer. Chem. Soc.*, **104** (17), p. 4759–4766.
[38] Kaptein, R. (1972). *J. Amer. Chem. Soc.*, **94** (18), p. 6269–6280.
[39] Musin, R. N. and Schastnev, P. V. (1976). *Jurn. Struct. Khimii*, **17** (3), p. 419–425.
[40] Trozzolo, A. M. (1968). *Acc. Chem. Res.*, **1** (1), p. 329–335.
[41] Gibbons, W. A. and Trozzolo, A. M. (1966). *J. Amer. Chem. Soc.*, **88** (1), p. 172–173.
[42] Barcus, R. L., Wright, B. B., Leyva, E. and Platz, M. S. (1987). *J. Phys. Chem.*, **91** (24), p. 6677–6683.
[43] Wright, B. B. and Platz, M. S. (1983). *J. Amer. Chem. Soc.*, **105** (3) p. 628–630.
[44] Wasserman, E. and Murray, R. W. (1964). *J. Amer. Chem. Soc.*, **86** (19), p. 4203–4204.
[45] Roebber, J. L. (1962). *J. Chem. Phys.*, **37** (9), p. 1974–1981.
[46] Davydov, E. Ya., Pariyskii, G. B. and Toptygin, D. Ya. (1977). *Vysokomolek. Soed.*, **A 19** (5), p. 977–983.
[47] Davydov, E. Ya., Pariyskii, G. B. and Toptygin, D. Ya. (1975). *Vysokomolek. Soed.*, **A 17** (7), p. 1504–1509.
[48] Davydov, E. Ya., Dobrovinskii, L. A., Pariyskii, G. B. and Toptygin, D. Ya. (1982). *Lakokrasochnye Materialy*, **3**, p. 15–17.
[49] Trozzolo, A. M., Murray, R. W., Wasserman, E. and Yager, W. A. (1962). *J. Amer. Chem. Soc.*, **84** (16), p. 3213–3214.
[50] Trozzolo, A. M. and Gibbons, W. A. (1967). *J. Amer. Chem. Soc.*, **89** (2), p. 239–243.
[51] Vorotnikov, A. P. and Davydov, E. Ya (1991). **10** (11), p. 1475–1479.
[52] Davydov, E. Ya., Vorotnikov, A. P. and Pustoshny, V. P. (1995). *Oxidation Communications*, **18** (3), p. 230–241.
[53] Mar'in A. P. and Shlapnikov, Yu. A. (1974). *Dokl. Akad. Nauk. SSSR*, **215**, p. 1160–1163.
[54] Kuzina, S. N. and Mihailov, A. I. (1976). *Dokl. Akad. Nauk. SSSR*, **231** (6), p. 1395–1398.
[55] Kovarskii, A. L., Placek, J. and Szocs, F. (1978). *Polymer*, **19** (9), 1137–1141.
[56] Vaserman, A. M. and Kovarskii, A. L. (1986). Spin labels and probes, Nauka, Moscow, p. 132–146.
[57] Grigor'eva, F. P. and Gotlib, Yu. Ya. (1968). *Vysokomolek. Soed.*, **A 10** (2), p. 339–348.
[58] Eisental, K. B., Turro, N. J., Sitzman, E. V., Gould, I. R., Hefferon, G., Langen, J. and Cha, Y. (1985). *Tetrahedron*, **41** (8), p. 1543–1554.
[59] Nikifirov, G. .A. and Ershov, V. V. (1979). *Mendeleev's JVHO*, **5**, p. 523–528.
[60] Baird, R. and Winstein, S. (1963). *J. Amer. Chem. Soc.*, **85** (5), p. 567–578.
[61] Vorotnikov, A. P., Davydov, E. Ya. and Toptygin, D. Ya. (1986). *Vysokomolek. Soed.*, **A 28** (9), p. 510–516.
[62] Roberts, J. D. and Caserio, M. C. (1964). *Basic Principles of Organic Chemistry*, Benjamin, New-York, p. 235.
[63] Tomioka, H., Ueda, H., Kondo, S. and Izawa, Y. (1980). *J. Amer. Chem. Soc.*, **102** (26), p. 7817–7918.

[64] Kudinova, P. I., Volod'kin, A. A. and Ershov, V. V. (1978). *Izv. Akad. Nauk SSSR, Ser. khimich.*, **7**, p. 1661–1663.
[65] Garrett, P. D. and Grubb, D. (1988). *J. Polymer Sci.*, **26** (12), p. 2507–2523.
[66] Lipatov, Yu. S. (1977). Fizicheskaya khimiya napolnennyh polimerov, Moscow, Khimiya, p. 304.
[67] Bryk, M. T. (1989). Destructsiya napolnennyh polimerov, Moscow, Khimiya, p. 191.
[68] Mardaleyshvili, I. R., Kutyrkin, V. A., Karpuhin, O. N. and Anisimov, V. M. (1979). *Vysokomolek. Soed.*, **B 21** (10), p. 834–836.
[69] Barnard, D. and Lewis, P. (1988). Natural Rubber Science and Technology. ed. A. D. Roberts, Oxford University Press, Oxford, p. 130.
[70] Kaplan, M. L., Kelleher, P. G., Bebbeington, G. H. and Hartless, R. (1973). *J. Polymer Sci., Polymer Lett, Ed.*, **11** (6), p. 357–361.
[71] Davydov, E. Ya., Pustoshnyi, V. P. and Vorontnikov, A. P. (1994). *Polymers and Polymer Composite*, **2** (6), p. 387–390.
[72] Ershov, V. V., Nikiforov, G. A. and Volod'kin, A. A. (1972). Space-hindered Phenols, Khimiya, Moscow, p. 204.
[73] Horswil, E. C. and Ingold, K. U. (1966). *Canad. J. Chem.*, **44** (3), p. 263–268.
[74] Roginskii, V. A. Kinetika I Kataliz (1982). **24** (9), p. 1808–1827.
[75] Howard, J. A. and Ingold, K. U. (1965). *Canad. J. Chem.* **43** (10), p. 2724.
[76] Shanina, E. L., Roginskii, V. A. and Zaikov, G. E. (1986). *Vysokomolek. Soed.*, **A 28** (9), p. 1971–1976.
[77] Roginskii, V. A., Dubinskii, V. Z. and Miller, V. B. (1985). *Izv. Akad. Nauk SSSR, Ser. khimich.*, **6**, p. 2808–2812.